ANALYSIS OF IPR CURVES IN NORTH SLOPE HORIZONTAL PRODUCERS SUPPORTED BY WATERFLOOD AND WATER ALTERNATING GAS EOR PROCESSES

By

Alan Abel, B.S. ChemE.

A Project Submitted in Partial Fulfillment of the Requirements

for the Degree of

Master of Science

in

Petroleum Engineering

University of Alaska Fairbanks

May 2019

APPROVED:

Obadare Awoleke, Committee Chair
Yin Zhang, Committee Member
Abhijit Dandekar, Committee Member and Chair
Department of Petroleum Engineering

Abstract

The shape and behavior of IPR curves in waterflooded reservoirs has not previously been defined despite their common use for optimization activities in such systems. This work begins to define the behavior of IPR curves in both water flood and water-alternating-gas EOR systems using a fine scale model of the Alpine A-sand. The behavior of IPRs is extended to 3 additional reservoir systems with differing mobility ratios. Traditionally derived (Vogel, Fetkovich) IPR curves are found to be poor representations of well performance and are shown to lead to non-optimal gas lift allocations in compression limited production networks. Additionally, the seemingly trivial solution to gas lift optimization in an unconstrained system is shown to be more complex than simply minimizing the bottom hole pressure of the producing well; maximized economic value is achieved at FBHPs greater than zero psi.

Table of Contents

List of Figures

List of Tables

1. Introduction

Most oil wells are not naturally flowing relying (Daleel 2015) on some form of artificial lift to reduce their flowing bottom hole pressure and increase draw down on their respective reservoirs. Gas lift is a common choice in offshore and arctic environments where reliability and ease of intervention are highly valued. The Alaskan North Slope is no exception where the great majority of producing wells are gas lifted; 100% of the ≈100 active producers of the Alpine Operating Area and 96% of the ≈500 active producers of the Kuparuk Operating Area are gas lifted.

Wells across an operating area produce into a shared production system with 1 or more centralized processing plants which have limited compression capacity. The constraint on compression capacity complicates the optimization of lift gas allocations. In an unconstrained system, the allocated lift gas of each well could be increased until a minimum bottom hole pressure was achieved. In a constrained system, the value of the incremental volume of gas allocated to any specific well needs to be weighed against the value it would produce if supplied to any other well of the shared production system. A thorough review of published gas lift optimization strategies was prepared by Rashid et. al. (2012).

Optimizing the marginal oil benefit of added lift gas across a shared production system is commonly called the "Incremental GOR Method" (IGOR). Weiss et. al. (1990) provide a detailed explanation of how this methodology has been applied at the Kuparuk field. They give credit for the original concept to the work of Redden et. al. (1974) who recognized that an algorithm which makes the change in benefit response to lift gas allocation equal across all wells would provide an optimum solution. Weiss et. al. (1990) developed a proof to show this was mathematically true for any number of wells when their performance curves (i.e. oil rate vs lift gas rate) are convex, see

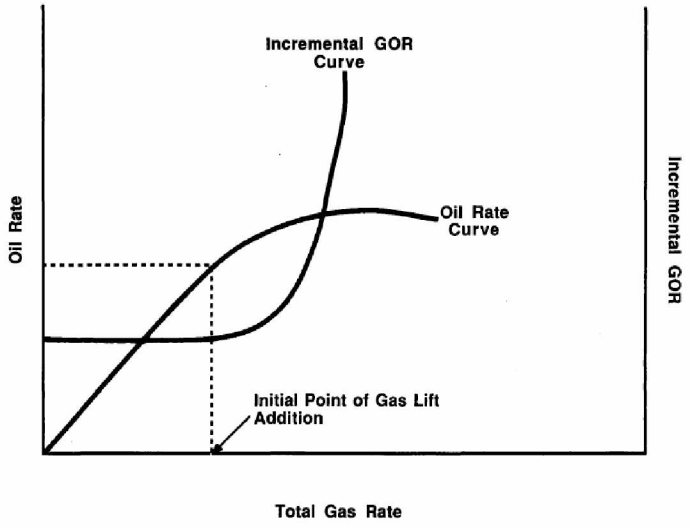

Figure 1.

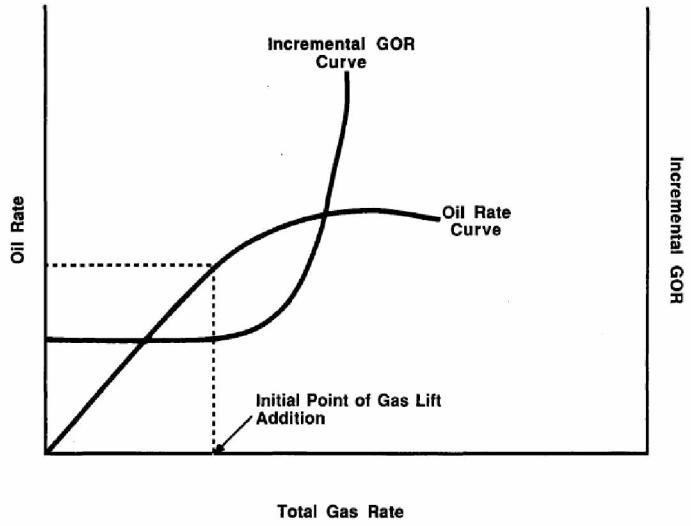

Figure 1: Well Performance and IGOR Curve (Weiss et. al. 1990)

The IGOR algorithm is still the primary method for gas lift optimization used in North Slope fields. If the producing oil field is thought of having two halves, reservoir deliverability and production capacity, efforts to improve the algorithm have been squarely focused on the production capacity half of the total system. These efforts revolve around better incorporation of impacts to the network itself: pressure drop in flow lines, the resulting wellhead pressure at each producer, and its effect on the lift curve for that well; inlet separator pressure and its effect on the network; and potential for more severe slugging into the processing facility. The first half of the total system, reservoir deliverability, has not received significant attention.

Classically, reservoir deliverability has been defined as an "inflow performance relationship" (IPR) curve. In its most simple form the IPR curve can be represented as a straight line, except for special cases this is generally considered to be an incorrect representation. In their seminal papers Vogel (1968) and Fetkovich (1973) provided the industry with non-linear representations of reservoir deliverability and, perhaps most importantly, documentation as to their applicability across a wide spectrum of vertical wells in solution gas drive reservoirs. The key characteristics of an IPR curve and the basic concepts of nodal analysis as it pertains to the performance of an individual well are depicted in Figure 2. The IPR curve extends from the y-intercept at a flow rate of zero to the x-intercept at an absolute open flow (AOF) rate. The y-intercept, zero flow rate point, occurs when the bottom hole pressure is equal to the reservoir pressure. Conversely the maximum possible rate

occurs at the x-intercept where the bottom hole pressure is zero. In the case of an under saturated oil reservoir the IPR curve is, generally considered to be, linear until the flowing bottom hole pressure drops below the fluid bubble point where the curve becomes non-linear and further reductions in bottom hole pressure result in a smaller oil rate response. The intersection of the tubing curve (also called a vertical lift curve) and the IPR curve represents the solution to the system and is the expected operating point for the well.

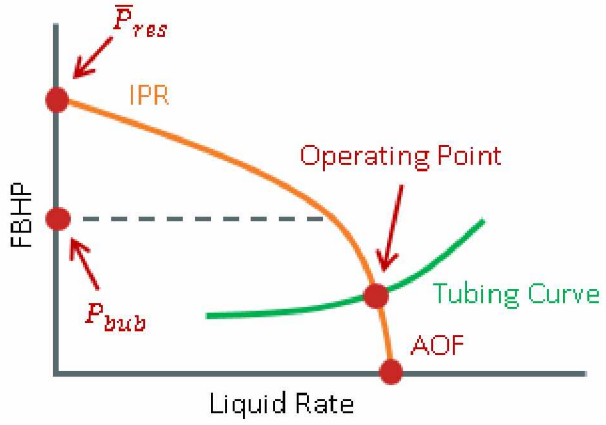

Figure 2: Representation of Classic IPR Theory for an Under Saturated Oil Reservoir

The addition of lift gas to the well system will tend to shift the tubing curve down, see Figure 3, creating a new operating point at a lower flowing bottom hole pressure. A break over point exists where too much lift gas will cause the frictional pressure drop in the production tubing to become greater than the reduction in gravitational pressure achieved by the lift gas' reduction in bulk fluid density. In this case the tubing curve will shift up with increasing amounts of lift gas.

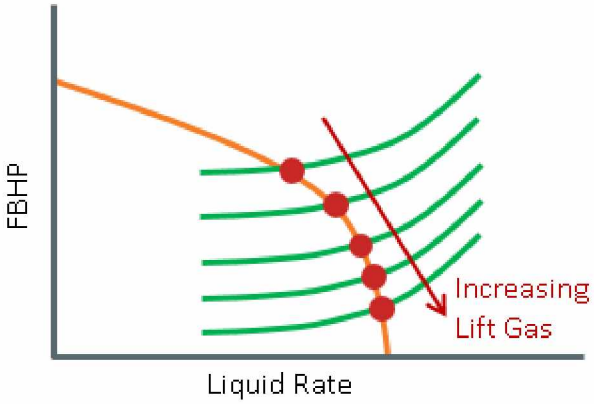

Figure 3: Effect of Lift Gas on the Tubing Curve

The operating points achieved by adding lift gas trace out a curve representing oil rate as a function of lift gas, the hypothetical operating points and the resulting oil rate benefit curve are shown in Figure 3

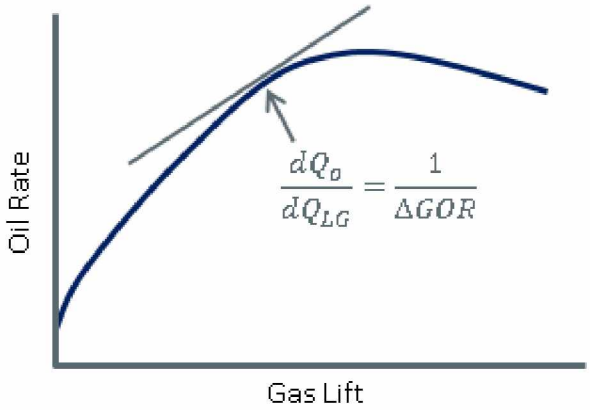

and

Figure 4 respectively.

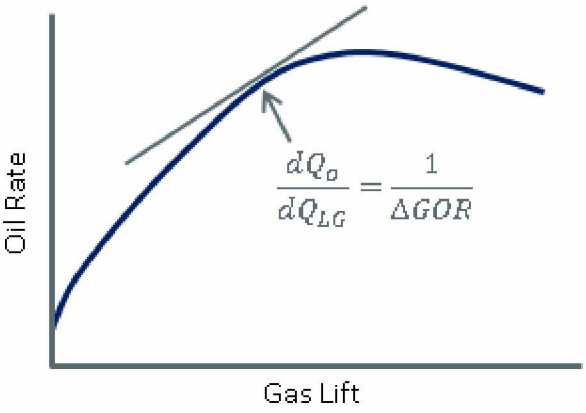

Figure 4: Oil Benefit Curve

The reciprocal slope of the oil benefit curve, accounting for produced gas volumes, yields an incremental GOR (ΔGOR) curve as a function of gas lift rate for each well as depicted in

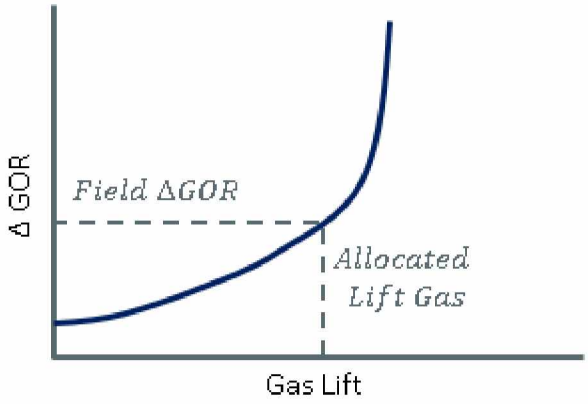

Figure 5.

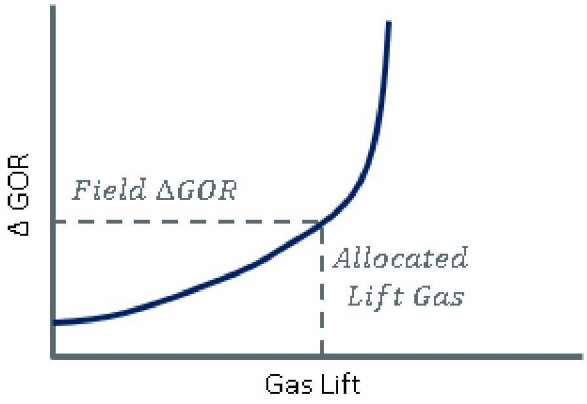

Figure 5: Incremental GOR Curve

The field level ΔGOR is then increased or decreased until the total required lift gas meets compression capacity.

The shape of the oil rate benefit curve, and thus the ΔGOR function, is a combination of the tubing and IPR curves. Since the tubing curves are generated from a correlation or multiphase flow model their shape and position in the solution space are not subject to much 'fitting' by the production engineer (assuming they have not grossly warped the models). In practice, it is the shape and position of the IPR curve that is manipulated to meet the perceived behavior of the well. Allocation of lift gas is, by and large, driven by the chosen shape of the IPR curve.

I reviewed the progression of IPR curves generated from initial production through to present day for producers in the Alpine field. Data from this field are readily available to me, frequent references back to it will be made through out this work, a description of the field can be found in Section 3.1. An example of this is shown in

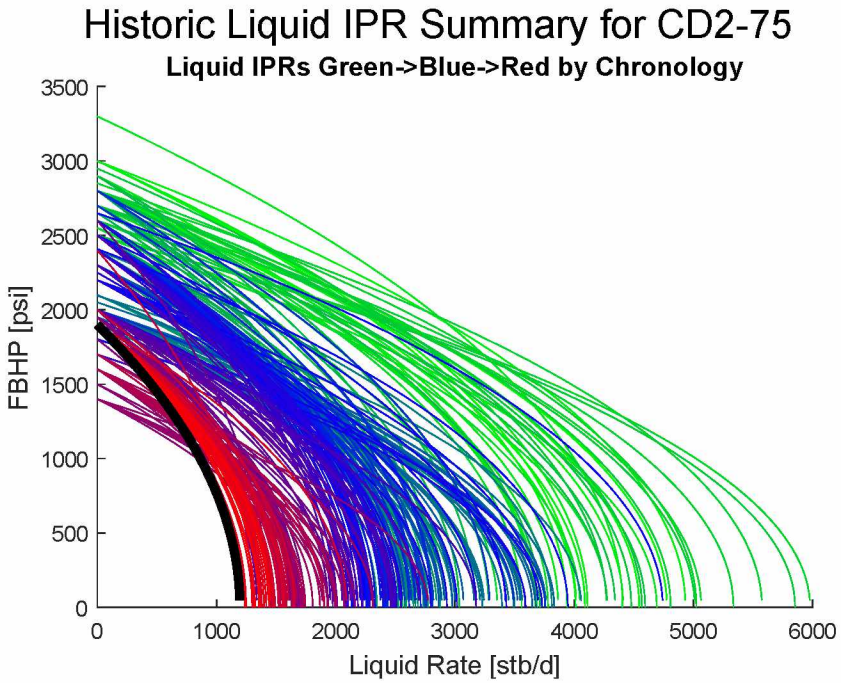

Figure 6, the color assigned to each IPR curve represents when in the life of the well it was created with the first IPRs in bright green progressing to blue and red in present day with the current active IPR in black. Well X is a horizontal producer flanked on either side by injectors, it has been under WAG flood since it was brought online and is representative of most of the producers in the Alpine field. The implied average reservoir pressure of each IPR curve from Well X is plotted against time in Figure 7. Being well supported with injectors, it is curious that the average reservoir pressure is consistently declining in time. This was a shared finding across the great majority of the field's producers. Full field reservoir simulation and material balance of the region estimate the current average reservoir pressure to be between 3,200 and 3,600 psi which is in clear disagreement with the y-intercept of the latest IPR curve at 1,900 psi.

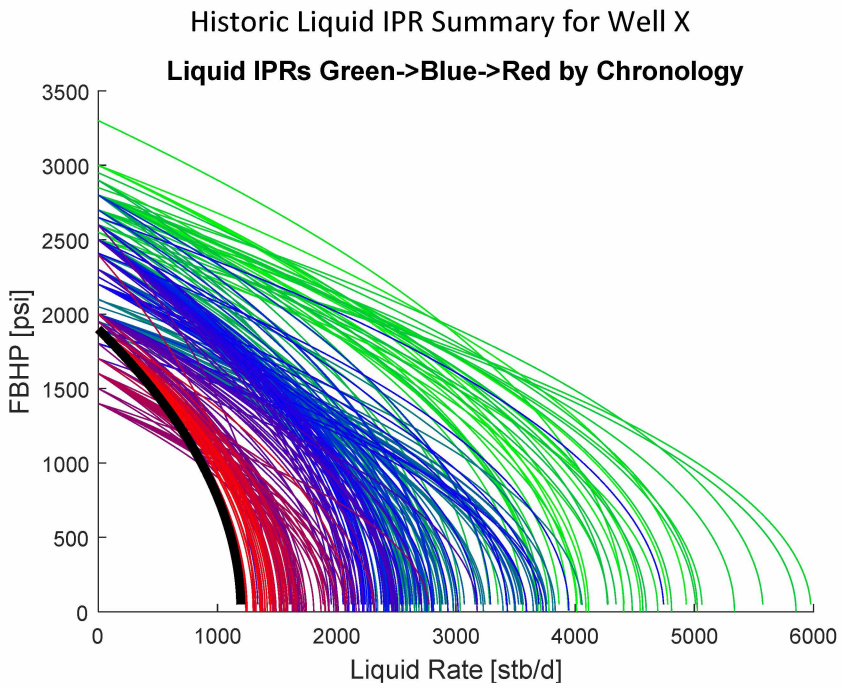

Figure 6: IPR Curves Generated for Well X of the Alpine Field

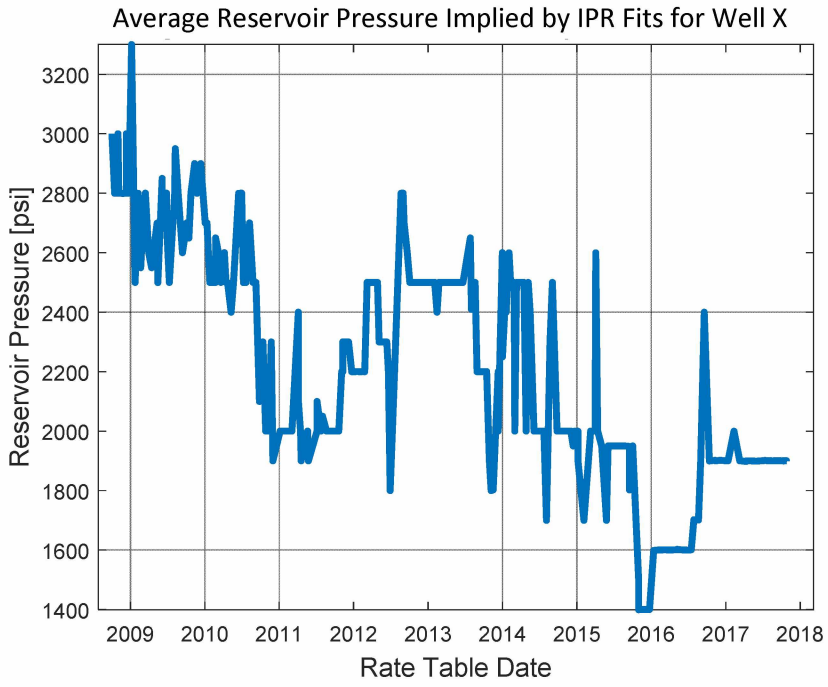

Figure 7: Average Reservoir Pressure Implied by IPR fit for Well X of the Alpine Field

Well X has been assigned to at least 5 different production engineers over its history, each engineer felt the best representation of the well's behavior was achieved by keeping the y-intercept below what

would be considered a reasonable reservoir pressure for a fully supported producer.

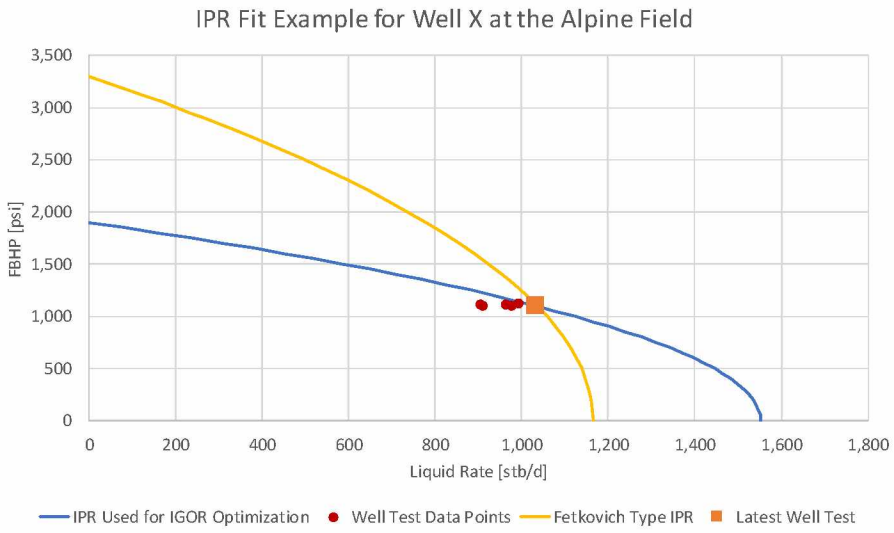

Figure 8 depicts the well test data used to make the latest IPR for Well X, the most recent well test is shown as an orange square with the 4 prior well tests as red circles. The latest IPR is shown as a blue line. It has become customary at Alpine to build all IPR curves from the Fetkovich function with the 'n' parameter equal to 1. With 'n' set, fitting the curve through the latest well test data requires specifying a low average reservoir pressure. A Fetkovich curve with n=1 and a more reasonable reservoir pressure at 3,300 psi set through the latest well test data point is shown as the orange line. The impact of average reservoir pressure on the slope of the resulting IPR curves is striking.

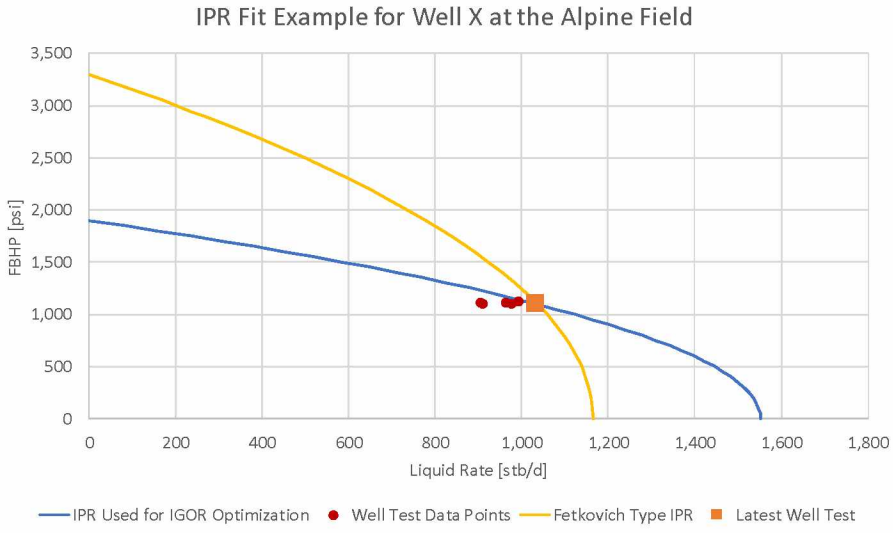

Figure 8: IPR Fit Example for Well X

As discussed previously the shape and position of the IPR curve is the primary driver of the resulting oil rate benefit curve. This concept of a 'steeper' sloped vs a more 'shallow' sloped IPR is depicted in

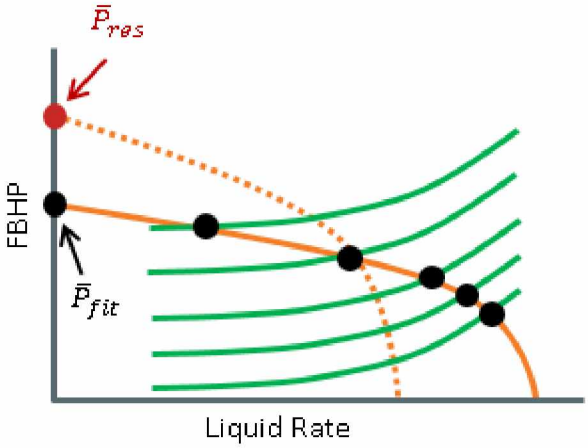

Figure 9 and the resulting ΔGOR curves are shown in Figure 10.

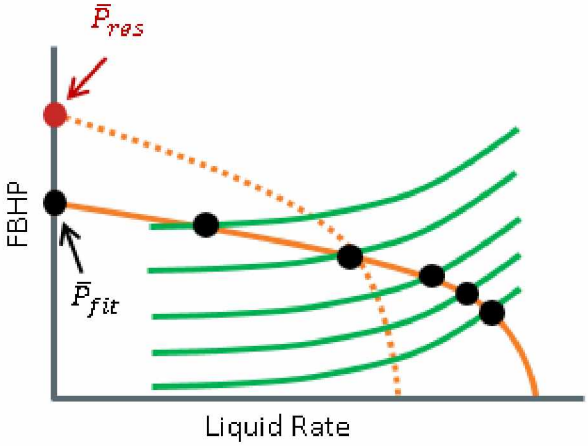

Figure 9: 'Shallow' and 'Steep' IPR Impact on Theoretical Operating Points

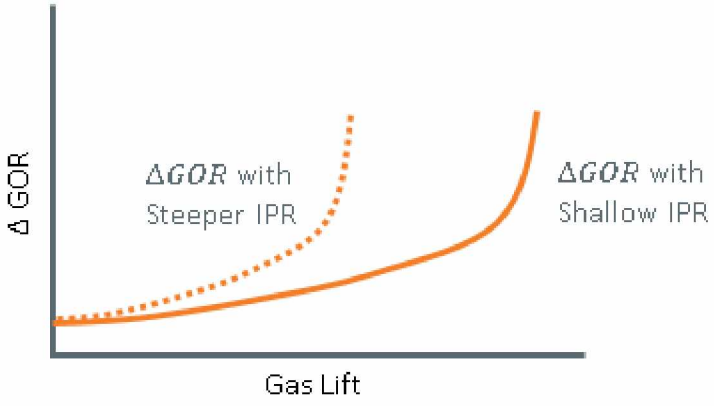

Figure 10: Resulting Incremental GOR Functions from Shallow and Steep IPRs

The ΔGOR curve generated from the shallower IPR curve will place more value (more oil benefit) to an added volume of lift gas vs the ΔGOR curve generated from the steeper IPR. This has far ranging implications on the short and long term operating decisions. What is the optimum allocation amongst currently producing wells? How much compression capacity should be dedicated to lift gas circulation vs bringing a shut-in well back on line? What is the true value of facility debottlenecking opportunities? The specific wells tests used for fitting, if the curve should be fit through all of them or a most recent representative test, and the method of fitting is left up to the assigned production engineer with little guidance on the expected behavior of the well. If we want the created IPR curves to be more consistent across each well and conform more to the expected behavior of the reservoir more formal and specific guidance needs to be provided to the production engineers.

Many studies have been conducted on the behavior of IPR curves in reservoirs being depleted under primary recovery (solution gas drive). This is not the way modern oil fields of any significant size are produced, if not available at field startup injection support will be provided shortly thereafter. A literature review of the subject found no specific material addressing the behavior of IPRs in a reservoir undergoing secondary or tertiary recovery. This work seeks to broaden, at least in some small way, the understanding of IPR behavior in water flooded reservoirs developed with horizontal wells as is now common in most developments. It is hoped that an improved understanding of IPR behavior in these types of developments will provide better guidance to the practicing production engineer on how to construct a representative IPR.

2. Review of Inflow Production Relationship (IPR) Curves

The arrival of the 1930's brought to the oil industry an appreciation for the amount of resource wasted by common operational practices, the value squandered with haphazard development strategies, and how both problems could only be solved with a better understanding of the physical processes governing petroleum systems (Coleman 1930, RRC 2017, occeweb 2017). In 1929 Coleman, Wilde, and Moore began to outline the basic physical relationships likely at play and what data must be gathered over the producing life of the reservoir to give a complete picture of potential rate and ultimate recovery (Coleman 1930); their work included outlining a proportionality between reservoir pressure and production rates, a simple volumetric method to calculate decline

in reservoir pressure as a function of produced volumes, and an approach to determine how much pressure support can be expected from re-injection of the produced gas.

Only 1 year later, in 1930, Moore details an experimental procedure to calculate the pressure-rate relationship he had previously left with only a qualitative description. First a well's shut-in pressure is measured to set the effective reservoir pressure, then the flowing bottom hole pressure is measured at several flow rates. He details how a plot of the reservoir-wellbore differential pressure vs the well's rate yields a line whose reciprocal slope is the productivity index defined in units of stb/d/psi (Moore 1930).

Several years later M.L. Haider published what may have been the first ever review of "present-day" IPR methods (many similar papers would follow over the next 80 years). His 1936 article, "Productivity Index" (Haider 1936), covers open-flow potential, restricted flow potential, and the increasingly mainstream "productivity index". Haider correctly identifies the importance of flow path on measured rates, both to short term transients and over longer time horizons. He also points out that "There is a question as to whether the productivity index, as defined above, is a constant value for a given well at various rates of production." (Haider 1936) However, by 1937 Haider has seen enough data to convince himself "if the index is properly determined and errors in measurement of production and bottom-hole pressure are eliminated, that index…is a constant with rate of production" (Haider 1937).

This put Haider at direct odds with S. C. Herold who felt "productivity index defined as the barrels per day per pound pressure differential is not a constant with rate of production" (Haider 1936). Herold was correct here and proved prescient in 1930 when he identified that assessment of reservoirs and production potential required understanding of the mechanical forces driving production from a reservoir as well as the physics of fluid flow through porous media, two areas petroleum engineers of his day were lacking critical knowledge of. (Herold 1930) While he was conceptually correct, it is worth noting the specifics of Herold's proposed reservoir mechanisms (hydraulic, volumetric, and capillary control) and measure of productivity index in each type would not prove out. He believed an index defined as the rate divided by the square of the reservoir-wellbore pressure differential would yield a straight line (constant index) in reservoirs under hydraulic and volumetric control. For capillary control reservoirs, the rate would be divided by the pressure differential to the three halves power. Neither method yielded straight line indices. (Haider 1936) Haider would test both Herold and Moore's constructs for productivity index in his 1936

review. From the well producing data he reviewed, A constant Moore PI was claimed for wells B and C with a non-constant increasing value demonstrated in well A. The Herold method for volumetric/hydraulic control reservoirs yielded a straight line for wells A and B while the method for capillary control yielded a straight line on well E. Haider was dismissive of this result but seeing that well E is from a different reservoir than wells A and B this work alone does not prove Herold incorrect.

Also, in 1936, Kemler and Poole demonstrate how IPR curves can be used as part of a workflow to optimize the design of a well, tailoring it to the producing capacity of the reservoir (Kemler 1936). In their work, the IPR curve is assumed to be a linear function of pressure. They also detail the potential pitfall of building an IPR curve from transient data points, "The production rate which can be obtained from a well depends on both the history of the well immediately before the test is taken and on the length of time over which the test is made." (Kemler 1936) A plot of their analysis on one well is shown in Figure 11. A known transient rate is shown as point A well above the measured steady state IPR curve. They are curiously close to being able to show a modern nodal analysis plot of the well, the tubing curve should be plotted as a function of rate and flowing BHP instead of the measured surface pressure at each test point.

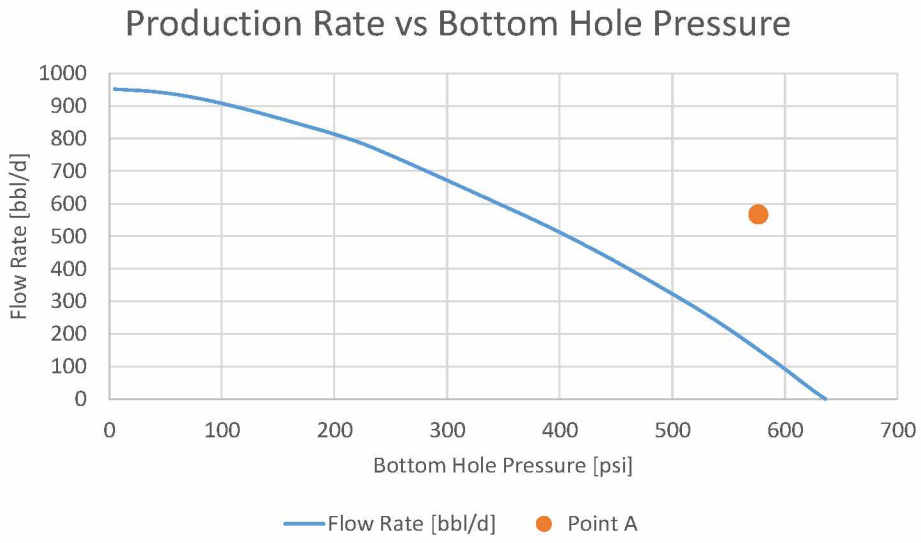

Figure 11: Plot of Production Rate and FBHP as Analyzed by Kemler and Poole (Kemler 1936)

In his 1938 review on reservoir productivity measurement (Walls 1938) Walls details the advancements made over the prior decade. He acknowledges the large published data set showing a generally linear trend in PI but takes care to point out the many, now, well established reasons one

should not expect it to be linear in all situations: under high flow rates the PI of a well could change due to the transition from viscous to turbulent flow; gas evolving from the oil; change in relative permeability from the change in saturation profile near the well bore; and in water-drive reservoirs an inability to support the flow rate with water injection. Walls demonstrates the observed inter-relationship of GOR and non-linear PI in

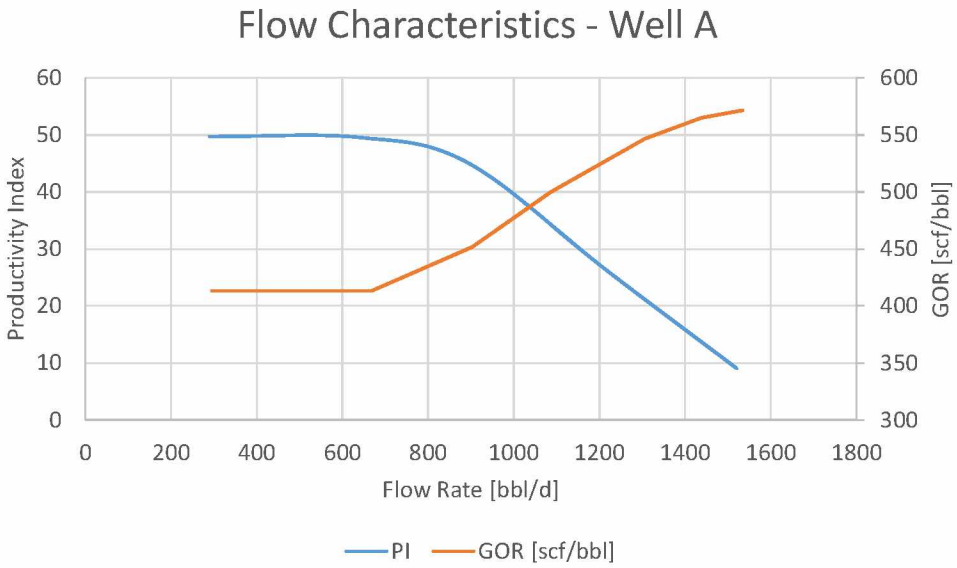

Figure 12.

Especially pertinent to the present work, Walls – for the first time in the reviewed literature – addresses the impact of water flooding. He explains, when at high flow rates, the rate of oil production may be limited by the influx of water, "the rate of water encroachment may be insufficient to maintain the productivity index constant" (Walls 1938). He also explores the impact of time, "there are logical reasons why it should vary in some cases and in others should remain approximately constant" (Walls 1938). Although he does not state this, you could easily replace "time" with "maturity" or "recovery". Scale up of experimental core flood data to something useful for field scale analysis is considered, an important concept for present day numeric models. The impacts of mud infiltration to the core, connate water saturations, relative permeability of oil and water are all explored. The limits of their current flow models are well understood (homogenous fluid, steady state, radial flow) and Walls gives a nod toward the future "Unfortunately, we are not entirely able at this time to set up quantitative expressions for the flow of all types of poly-phase systems through the range of porous materials encountered in oil reservoirs in terms of permeability, saturation, viscosity, and interfacial effects." (Walls 1938)

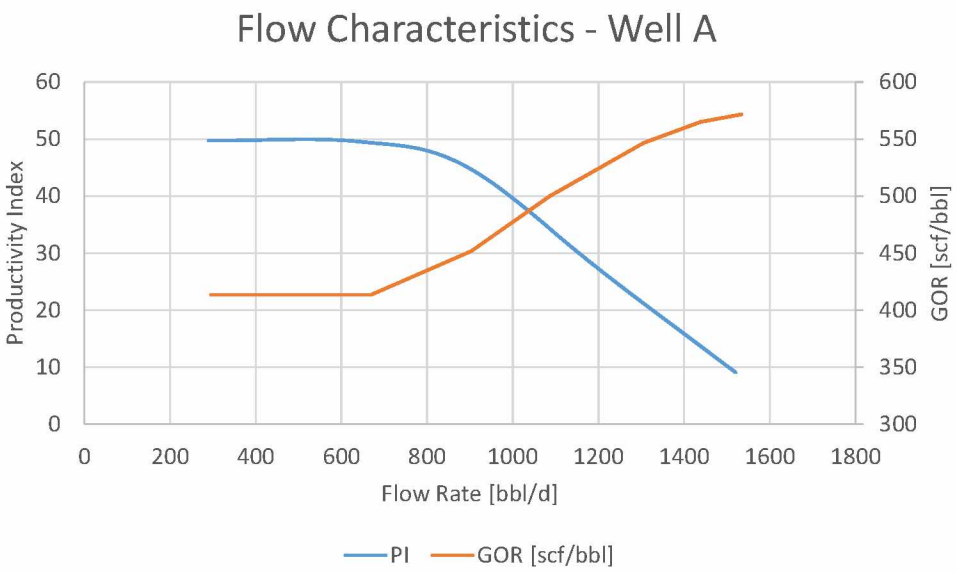

Figure 12: Walls' Diagram Relating Increased GOR with Non-Linear PI

By 1941 the theoretical analysis on the concept of PI had been sufficiently advanced and enough field data observed for Evinger and Muskat to write that a constant PI was an impossibility in any heterogeneous system and to suggest that the term, if a constancy is to be inherent in its definition, be limited to the "slope of the curve of flow rate vs. pressure differential as the pressure differential is made vanishingly small" (Evinger 1942). They also make note that maintaining long term steady state within a heterogeneous fluid system is an impossibility unless the system is under waterflood in which case a constant pressure boundary is possible but would be moving. This sentiment persists to the modern day though it is only true for the obscure case of an immiscible flood process occurring without any change to the relative permeability of the phases.

Vogel's seminal 1968 paper "Inflow Performance Relationships for Solution-Gas Drive Wells" is generally, among industry professionals, given credit for establishing a non-linear IPR curve and presenting the general shape (or fit) of this curve. Vogel's reference curve takes the normalized form of Equation 1.

$$\frac{q_o}{(q_o)_{max}} = 1 - 0.2\left(\frac{P_{wf}}{\bar{P}_r}\right) - 0.8\left(\frac{P_{wf}}{\bar{P}_r}\right)^2$$

Equation 1: Vogel's Normalized Reference Curve

The previously reviewed literature outlined above provides substantive evidence that researchers 25 years prior to Vogel were correctly demonstrating that the IPR curve was a non-linear function of flowing wellbore pressure and this non-linear behavior was strongly linked to increasing GOR. What Vogel did do, in programming Weller's analytical solution to gas-oil flow (whose significant advancement was allowing for varying GOR as a function of pressure) (Weller 1966), was provide the most rigorous solution yet to test IPR behavior in solution-gas drive systems and then provide a simple curve fit so the practicing engineer could apply it to their wells. Weller's two-phase flow solution allows demonstration that IPR curves change significantly as a function of recovery from the pattern as shown in Figure 13. Vogel's normalization of the IPR curve with dimensionless pressure on the x-axis and dimensionless rate on the y allows simplification of a large family of curves into one curve, see

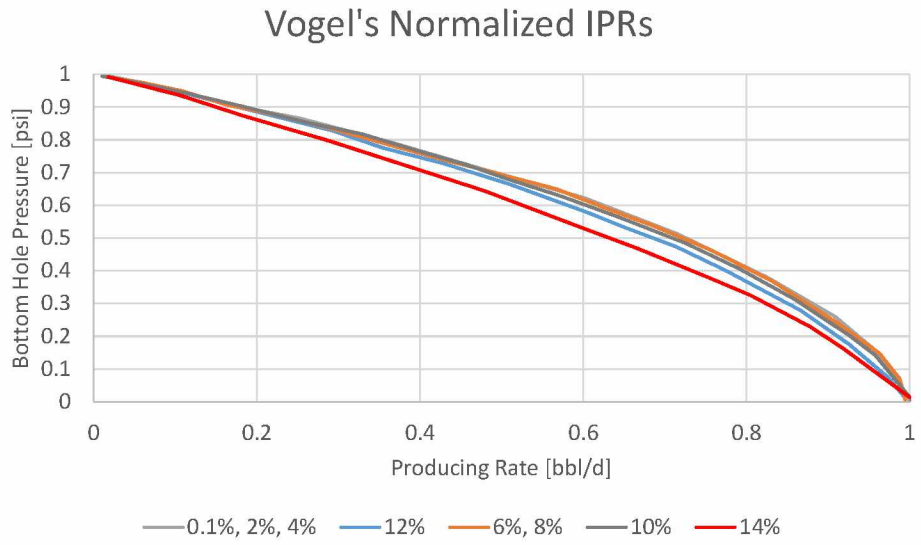

Figure 14. It is worth noting that the higher recovery IPRs, even when normalized, do not fit well with the low recovery curves. Of interest to this present work is Vogel's clear statement on the pitfalls of building IPR curves from multi-rate tests in low permeability reservoirs:

> "*It is difficult to overstate the importance of using stabilized well tests in the calculations. In a low-permeability reservoir it frequently will be found that significant changes in producing conditions should not be made for several days preceding an important test. This presents no problem if a well is to be tested at its normal producing rate, but it becomes more difficult if multi-rate tests are required.*" (Vogel 1968)

Vogel is also clear that his proposed IPR curve will need to be recalculated for reservoirs under another drive mechanism, exactly what this present work attempts to undertake.

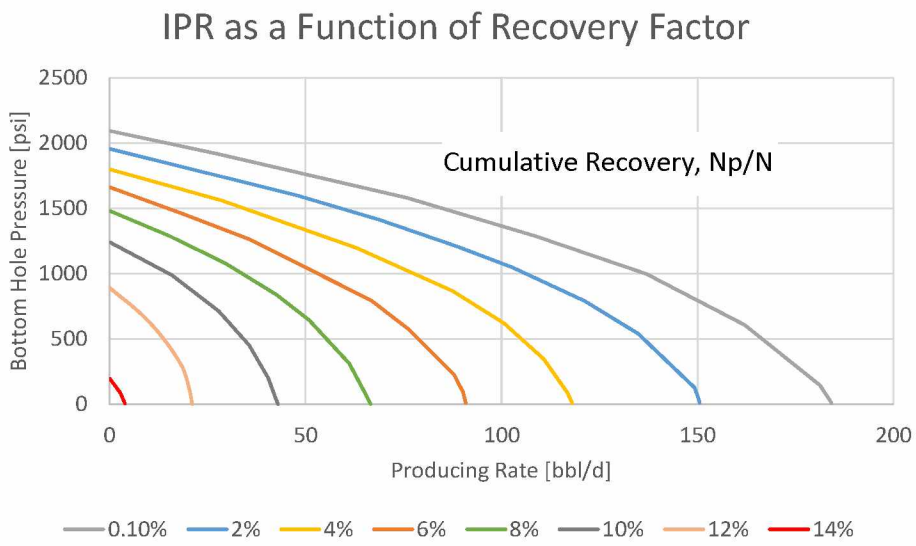

Figure 13: Vogel's IPR Curves as a Function of Recovery in a Solution-gas Drive Reservoir (Vogel 1968)

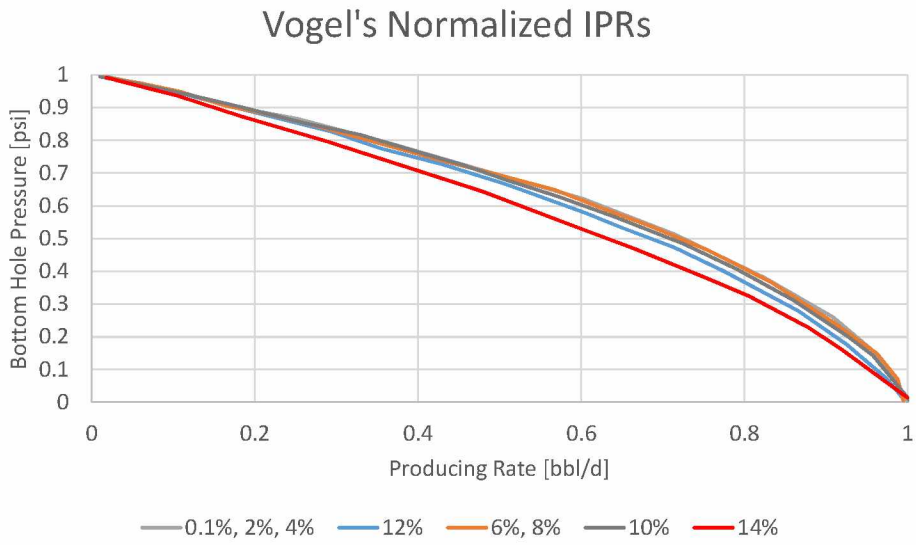

Figure 14: Vogel's Normalization of a Family of IPR Curves into a Single Curve (Vogel 1968)

Standing (1971) builds on Vogel's work by recognizing the role relative permeability will surely play on the IPR curves and proposing a method by which the empirical curve might be shifted as oil relative permeability changes in the system. This method does not re-solve the flow equations or use measured field data and should be considered highly approximate.

In 1973 Fetkovich published “The Isochronal Testing of Oil Wells” in which he proposes a new IPR curve and details results of its fit on multi-point drawdown tests of some 40 oil wells in reservoirs of widely varying permeability and fluid types. His new IPR simplifies the radial flow equation developed by Evinger and Muskat (1942) to a difference of squares, an exponent, and a coefficient (see Equation 2).

$$q_o = J'_o\left(P_e{}^2 - P_{wf}{}^2\right)^n$$

Equation 2: Fetkovich IPR Relationship

A

Figure 15. As with Vogel’s equation, given knowledge of the boundary pressure and governing exponent an IPR curve can be fit with a single well test data point. An exponent less than 1 (n<1) will be caused by the impact of gas-oil relative permeability and near wellbore non-Darcy flow in high rate wells. Fetkovich observed in his testing that the exponent obtained for oil wells in saturated reservoirs was consistently less than 1. The same should be expected of undersaturated reservoirs. On a general side note, to test for turbulent flow Fetkovich cites Muskat and uses the standard Reynolds number (with grain diameter as the characteristic dimension) with any value larger than 1 indicating non-Darcy turbulent flow

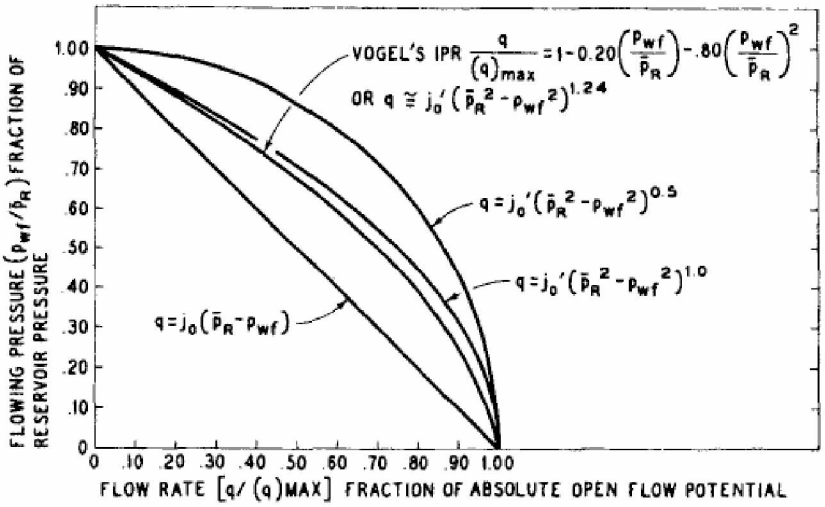

Figure 15: Comparison of Fetkovich, Vogel, and Linear IPR Curves (Fetkovich 1973)

The

Bendakhlia

Figure 16.

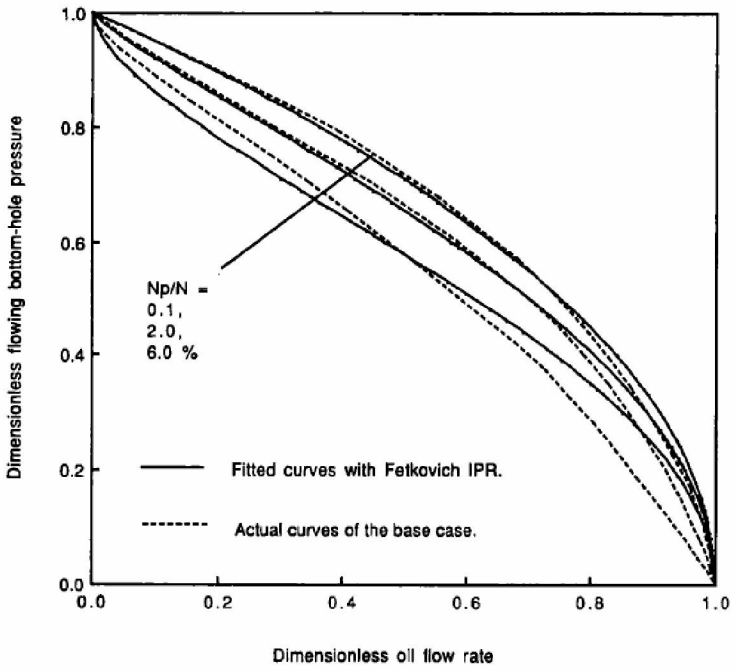

Figure 16: Fitting of Fetkovich IPR to Bendakhlia's Simulation Defined IPRs (Bendakhlia 1989)

The

Similar

In

Retnanto

In

A

More

3. Setup of Reservoir Model

3.1. Overview of the Alpine Reservoir

The

The

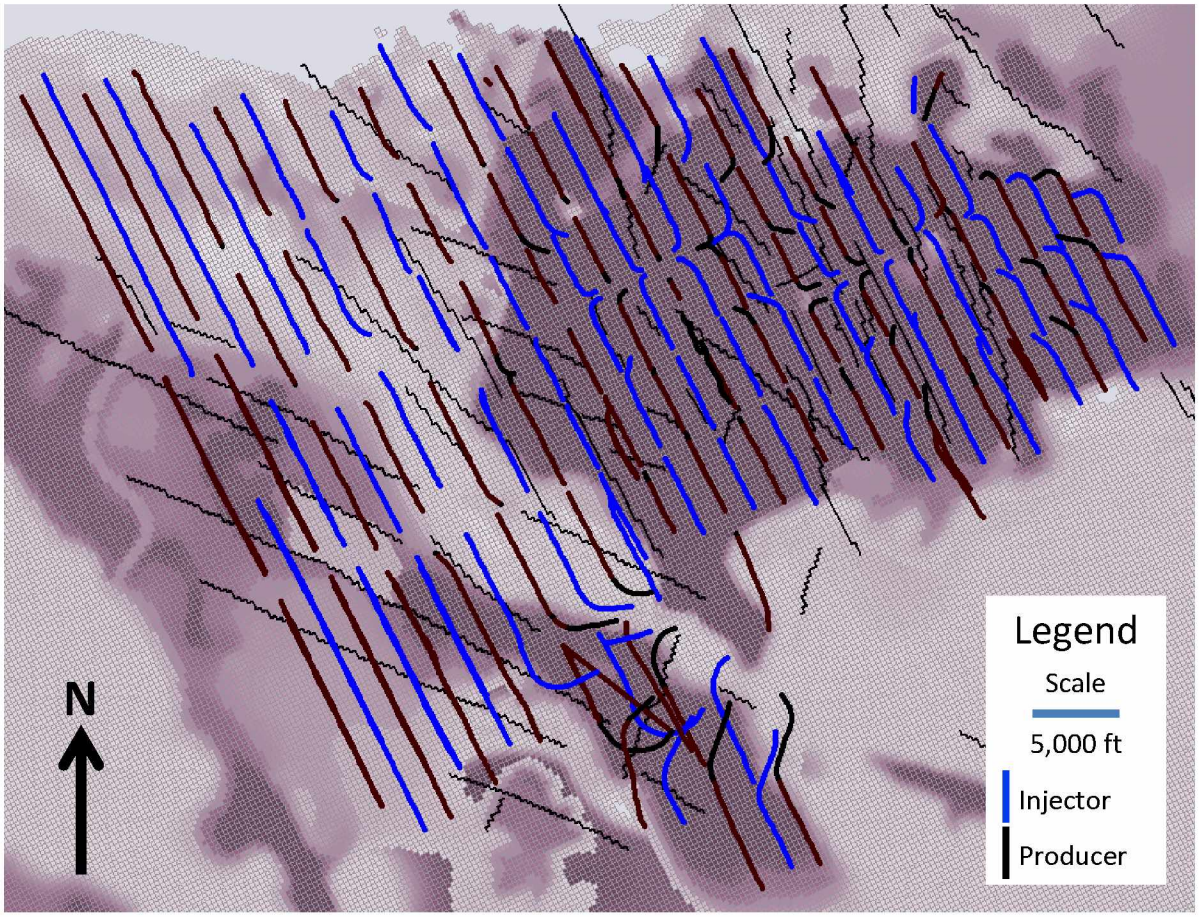

Figure 17: Alpine Field Map - Line Drive Development

3.2. Description of Type Pattern Model

The region represented by the type pattern model was chosen to be centered on a producer with nearly a decade of production history. This provides a large data set to 'back-cast' the model against (see below). Areal and cross section views of the sector model are shown in Figure 18.

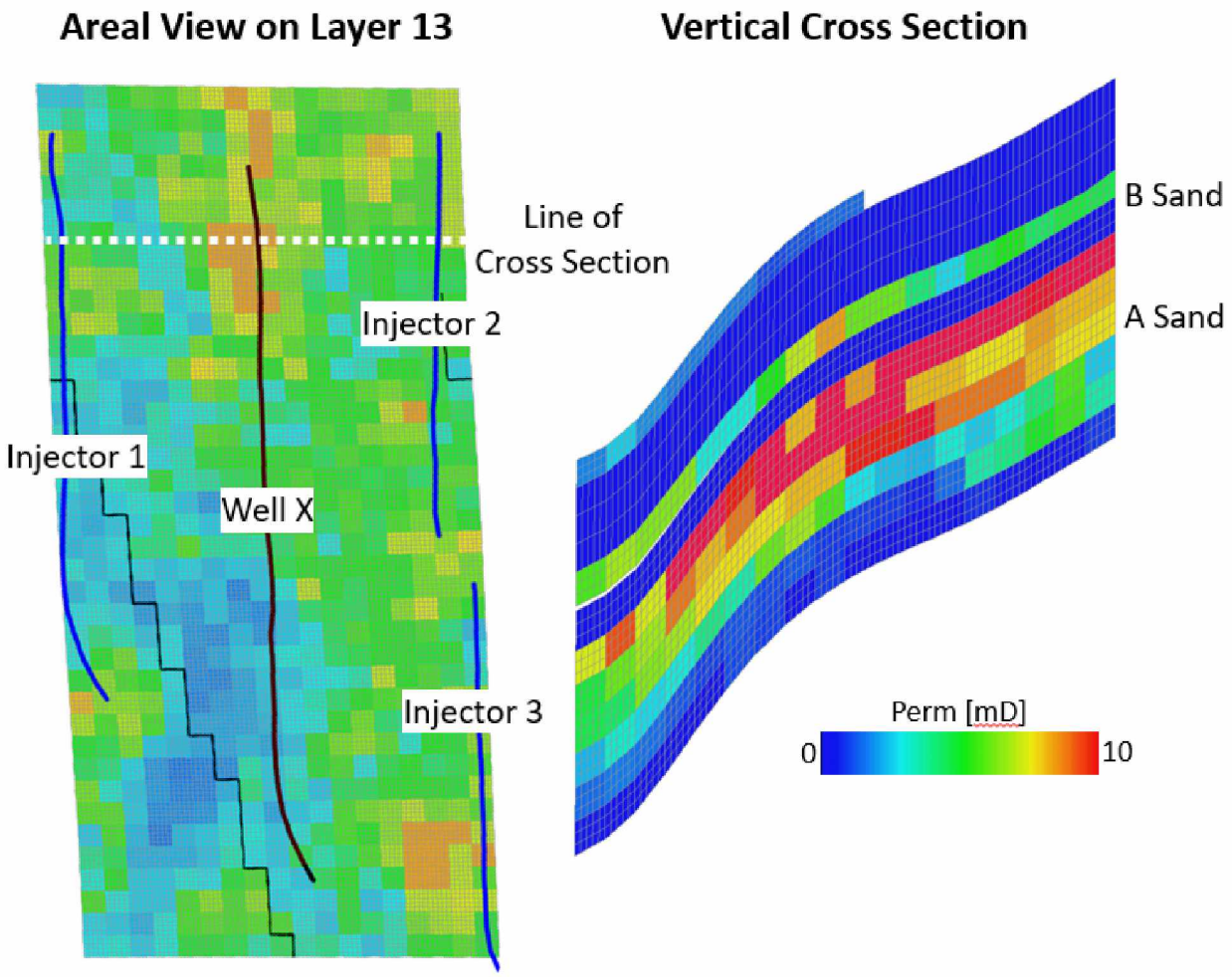

Figure 18: Views of Permeability Distribution in Fine Scale Sector Model

The

Modeling production wells follows the industry standard Peaceman formulation (Peaceman 1991) where the offtake is calculated as a function of wellbore to grid cell pressure differential, phase mobility, and a constant representing the combination of several static grid parameters, see $qp=$

$$PI\lambda_p(p_g - p_{wf})$$

Equation 3 below. In the common situation of a well completed in multiple cells, the model sums across all the completed grid cells to obtain the total phase rate.

$$q_p = PI\lambda_p(p_g - p_{wf})$$

Equation 3: Well Inflow Equation

When discussing wellbore models used in numeric reservoir simulation in the context of IPR curve analysis the concept of "PI" becomes muddled. The "PI" which refers to the slope of an IPR curve is not, inherently, related to the static proportionality used to calculate well rates in a numeric reservoir model. The "PI" used by reservoir models, also called the Well Index (WI) in an attempt to avoid this confusion, Equation 4, this paper will take care to clearly differentiate which PI is being discussed.

s

Equation 4, this paper will take care to clearly differentiate which PI is being discussed.

d

$$PI = \frac{2\pi kh}{\ln(r_0/r_w)}$$

e

f

i

n

Equation 4: Definition of Well Productivity Index

e

d

Peaceman's contribution to the modeling of wellbore inflow was the definition of the radius where the flowing wellbore pressure would be equal to the average pressure of the grid block assuming steady

i

state radial flow for the case of a non-square block. The original derivation of this radius was for

n

horizontal wells acting in an infinite reservoir. His result as adapted for horizontal wells is shown as $r0=$

$$0.28\frac{\left[\left(k_y/k_z\right)^{1/2}\Delta z^2+\left(k_z/k_y\right)^{1/2}\Delta y^2\right]^{1/2}}{\left[\left(k_y/k_z\right)^{1/4}+\left(k_z/k_y\right)^{1/4}\right]}$$

Equation 5. This adaptation is not based on a rigorous derivation, the direction of the permeability values is shifted to account for the new orientation of the wellbore. The horizontal orientation assumes an infinite acting reservoir. However, this is less valid when horizontal wells are drilled in thin sands where the top or bottom (or both!) boundaries of the reservoir may be just a couple feet away. This is a known weakness in the calculation of PI/WI in reservoir simulators which at present does not have a readily available solution.

$$r_0 = 0.28\frac{\left[\left(k_y/k_z\right)^{1/2}\Delta z^2+\left(k_z/k_y\right)^{1/2}\Delta y^2\right]^{1/2}}{\left[\left(k_y/k_z\right)^{1/4}+\left(k_z/k_y\right)^{1/4}\right]}$$

Equation 5: Peaceman Equation for Effective Well Radius (Peaceman 1991)

After 3 years of production, the modeled producer is fractured. The primary goal of this fracture was to access the B sands lying above the wellbore but not in pressure communication with it. The timing of the fracture is captured in the model, i.e. the completions of the producer are changed in time. There is uncertainty in position and size of the created fracture when stimulating an open hole horizontal well. To the best of our knowledge, a 250 to 500-foot-long fracture was created oriented along the axis of the well and centered about its heel. This is captured in the model by adding completions vertically into cells the well is not drilled through. Figure 19 shows how this fracture is represented in the sector model, the vertical pressure differential in the cross section makes the separation of A and B sands clear. The well's trajectory will cause some of the completions in the middle section of the lateral (highlighted boxes/cells) to appear out of the plane of view.

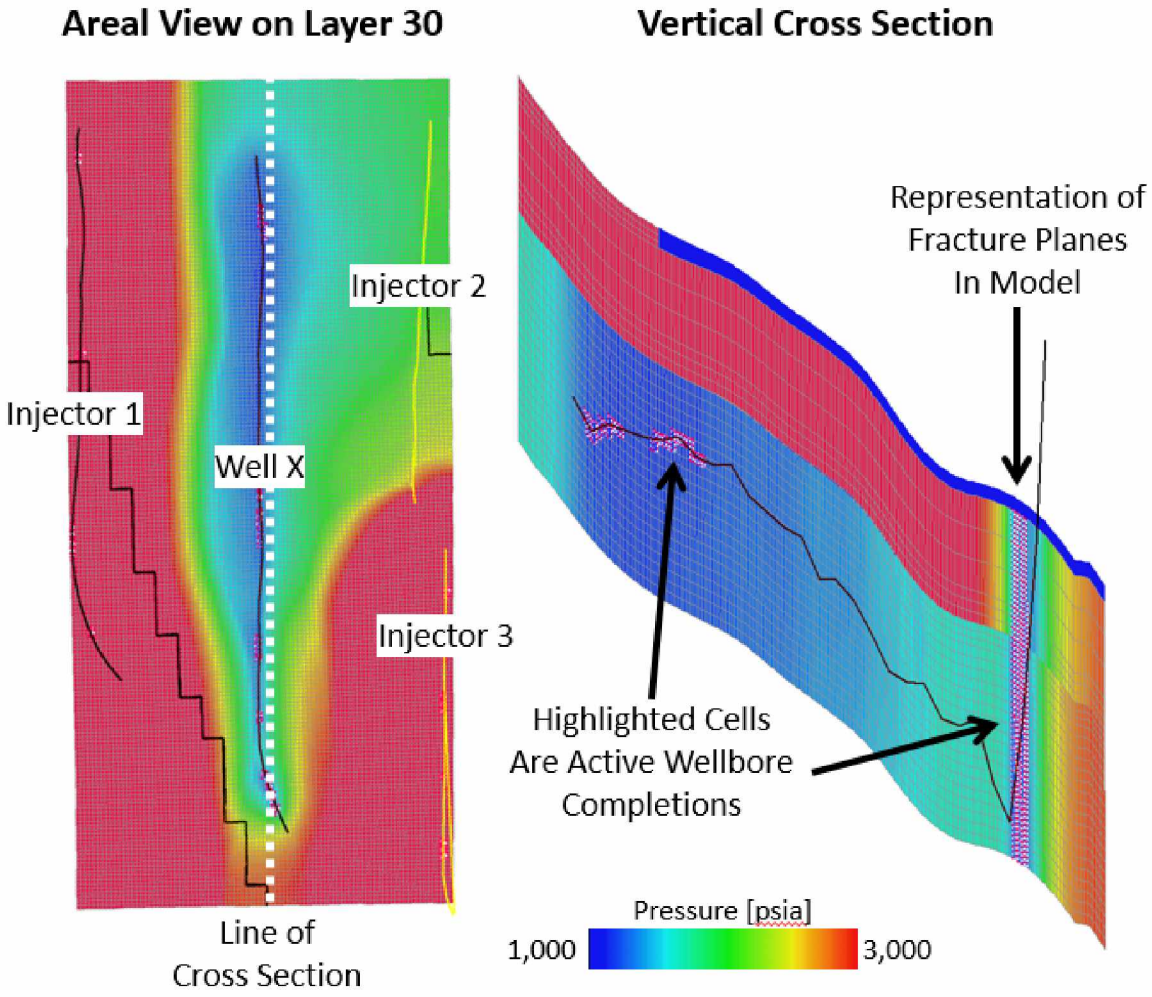

Figure 19: Representation of Producer Heel Frac in Sector Model

Alpine injection wells are not fractured with a conventional pump truck treatment, however their bottom hole pressure during water injection is above the fracture pressure of the reservoir matrix. In some instances, the water injection fractures can become large enough that a well will be in communication with another injector along its row; of interest in this work is the communication established between Injector 2 and Injector 3 (on the eastern side of the sector model). We primarily identify communication between injectors by shutting one in for an extended period then measuring its bottom hole pressure, if the bottom hole pressure is at or near the flowing bottom hole pressure of an adjacent well in the row then we can confidently determine that the two wells have a non-matrix flow connection. When injectors are switched to gas service their bottom hole pressures will fall below the fracture pressure of the reservoir. Fracturing on one service and not on the other has a significant impact on the behavior of the injection wells and must be accounted for in the sector model to achieve the level of fidelity desired when matching the dynamics of the pattern.

The treatment of water injection fracturing is similar to what was described for the producer. Completions are added above and below the wellbore to represent the fracture plane. Unlike the producer these completions extend along the full length of the wellbore and past the heel and toe. Figure 20 shows the representation of water injection fracturing for Well X in the sector model. When the well service is switched to gas the fractures are assumed to close and the injection will be limited to the drilled lateral. Figure 21 depicts the same well, Injector 1, on gas injection service. The well's trajectory will cause some of the completions toward the heel (highlighted boxes/cells) to appear out of the plane of view.

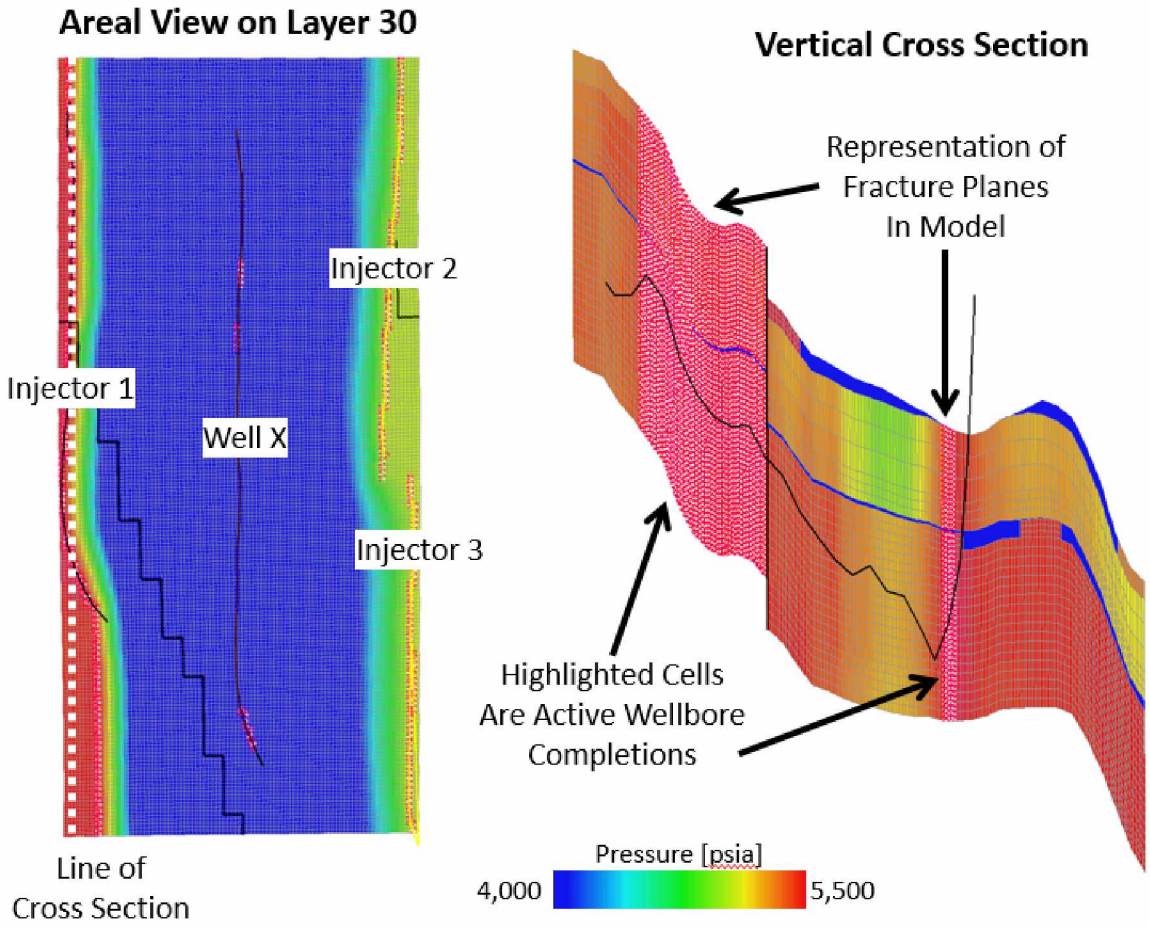

Figure 20: Representation of Water Injection Induced Fracturing in Sector Model

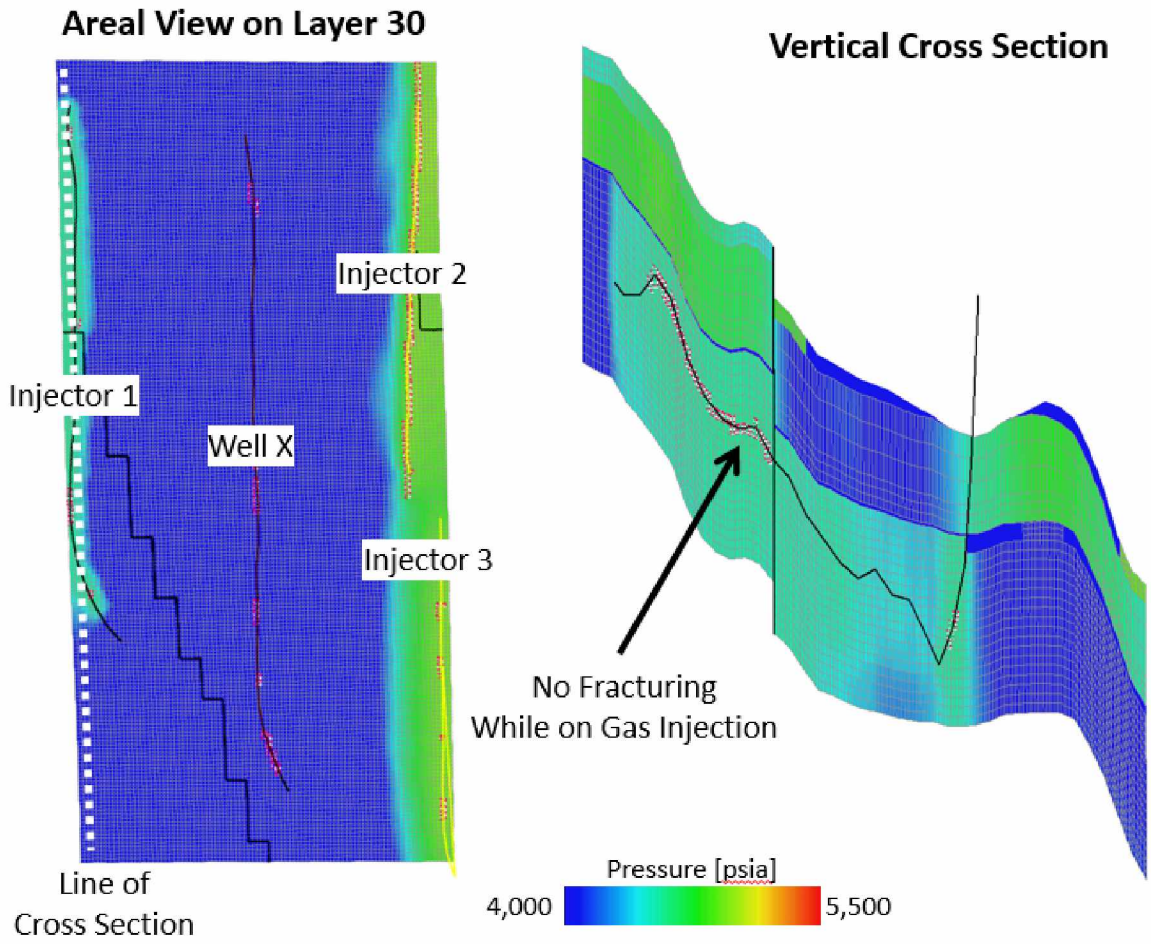

Figure 21: Injector Completions While on Gas

3.3. Back-Casting Validation of Sector Model

In a traditional history match the rates of injectors and producers are set to match the known measured rates. The simulator then calculates the bottom hole pressure required to achieve that rate. In a back-casted model the known bottom hole pressures are specified, and all rates are calculated by the model. This technique lends itself to a more natural understanding of the errors in the model. For instance, if a back-casted model is off 2% on cumulative oil production and 4% on cumulative water production the error is within the known accuracy of the metering system and the model would be considered to have an excellent match. On the other hand, if a rate specified model is off 0% on its oil and water cumulatives but has an average pressure error of 350 psi at each time step, should we consider the model to have a good match or a poor match? What is the impact of the error on the forecasted rates?

The back-casting approach has the additional benefit of giving a robust calculation of injector contribution to the producer centered pattern. Since the boundary of the model is set by the injectors, each injector is only ½ of a well, its other ½ lying outside of the boundary. In this case, it is not clear how much of the measured rate of the actual well to ascribe to the defined ½ well of the model. Since the back-casting approach uses only the known BHP, a value which does not change when the well is "divided", the rate allocation to the model is naturally calculated. Since the reservoir quality in the chosen region is like its surroundings, and the timing of wells being brought on production isn't too spread out, the total injection volume achieved by the flanking injector wells is expected to be in the 40% to 60% range.

A comparison of the modeled producer (Well X) performance to the observed performance follows below; the key point here is to show that the physical processes occurring in the reservoir are well captured by the model. Plots of oil rate and cumulative oil production in time are shown first in Figure 22 and Figure 23. Three events are highlighted on the plot of oil rate: an initial reduction in wellbore inflow PI (WI); a re-set of the wellbore PI to the Peaceman calculated value; and the point of fracture stimulation where a connection to the B sand was made. These three events are the only times the producer inflow model was altered. Justification for the initial PI reduction is based on the response observed just after the 'January 2009' date stamp where, following a brief shut-in, the well came back online with an obvious uptick in production. It would seem either a portion of the lateral was not initially contributing, or some kind of general impairment to well production had been removed. The most important feature of the oil rate profile is the decline in rate from 2013 through 2016 which captures the changing mobility of the system as the water flood front approaches the producer.

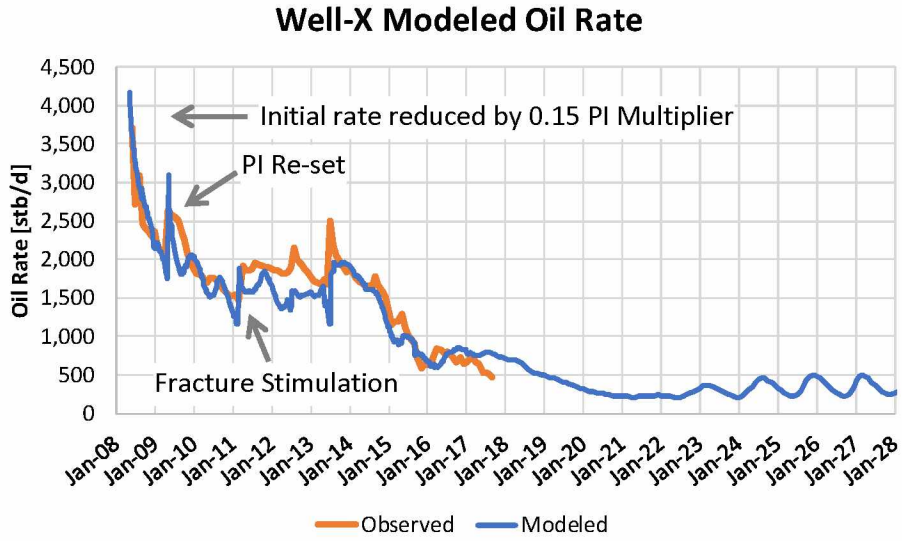

Figure 22: Sector Model Forecasted vs Observed Oil Rate

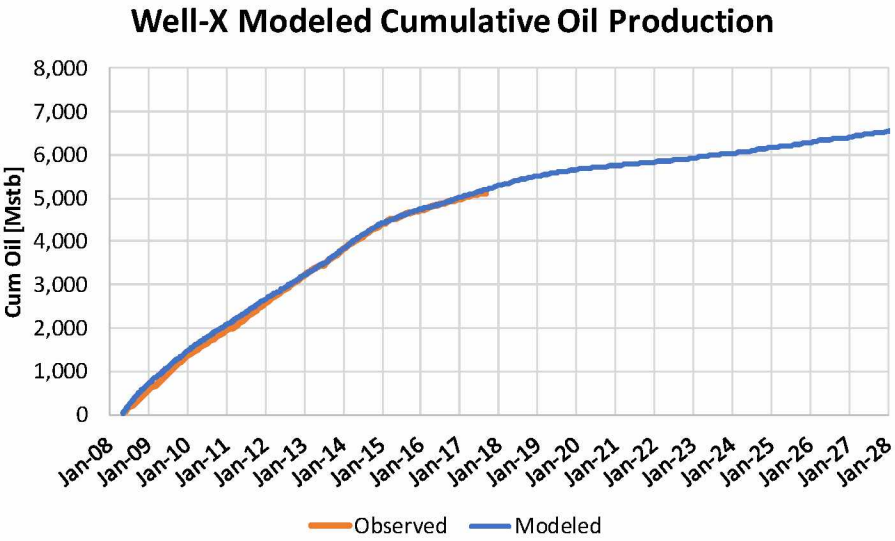

Figure 23: Sector Model Forecasted vs Observed Cumulative Oil Production

The cumulative oil production is well matched with an error of 1.5% through September of 2017. An excellent method for observing the mechanics of a waterflood is the dimensionless WOR performance plot where the WOR of a well is plotted as a function of its recovery factor. Figure 24 shows this for Well X, take note of the y-axis log scale which details initial water breakthrough behavior more than a Cartesian scale. The sector model does an excellent job of capturing the waterflood performance of the pattern.

Figure 24: Sector Model vs Observed WOR Performance

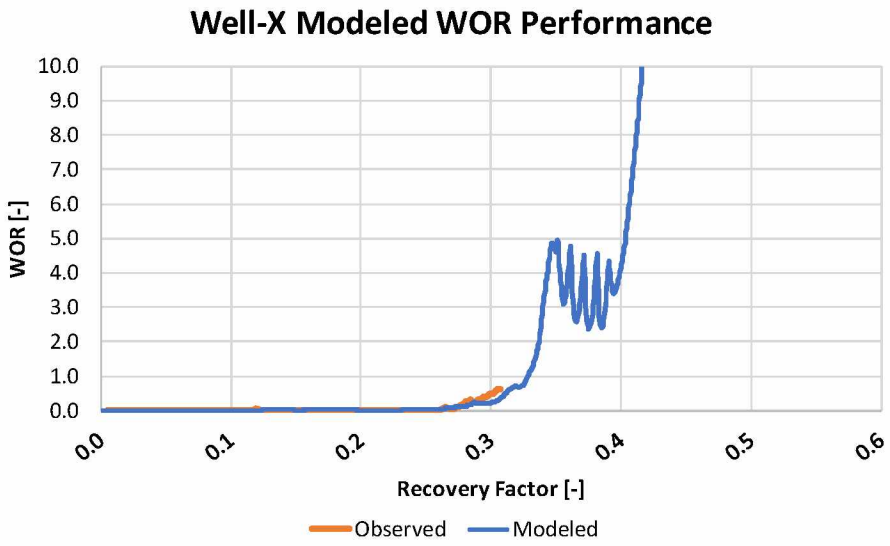

As opposed to the waterflood and liquid rate matches, the gas production match is poor. Figure 25 shows the match to observed data with an error of nearly 80%. This error has several possible causes: Well X is one producer in a line drive with two other producers located just north and south of it, the interactions with these producers are not captured with the sector model; the injectivity of the gas could be poorly captured by the model allowing too much gas to be injected at the specified bottom hole pressure; finally, the PVT of the system could be misrepresented and the true GOR of the system is lower.

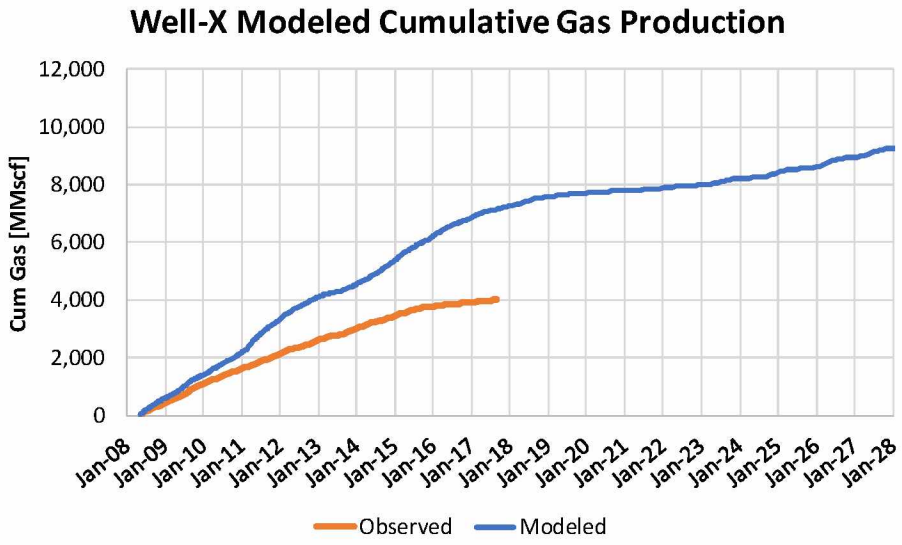

Figure 25: Sector Model vs Observed Cumulative Gas Production

Plots of cumulative water injection for each injector follow below. Table 1 shows the predicted allocations for water and gas volumes to the producer Well X. These are calculated as shown below in Equation 6. As stated previously, these values are expected to be 40-60%, a hurdle which the values in Table 1 largely meet.

$$\boldsymbol{Allocation}\ \% = \frac{\boldsymbol{Modeled\ Injection\ Volume}}{\boldsymbol{Historic\ Injection\ Volume}} * \mathbf{100}$$

Equation 6: Calculation of Injection Volume Allocation

Injector Well	Water Allocation	Gas Allocation
Injector 3	34%	60%
Injector 2	43%	46%
Injector 1	69%	50%

Table 1: Calculated Injection Volume Allocations to Well X

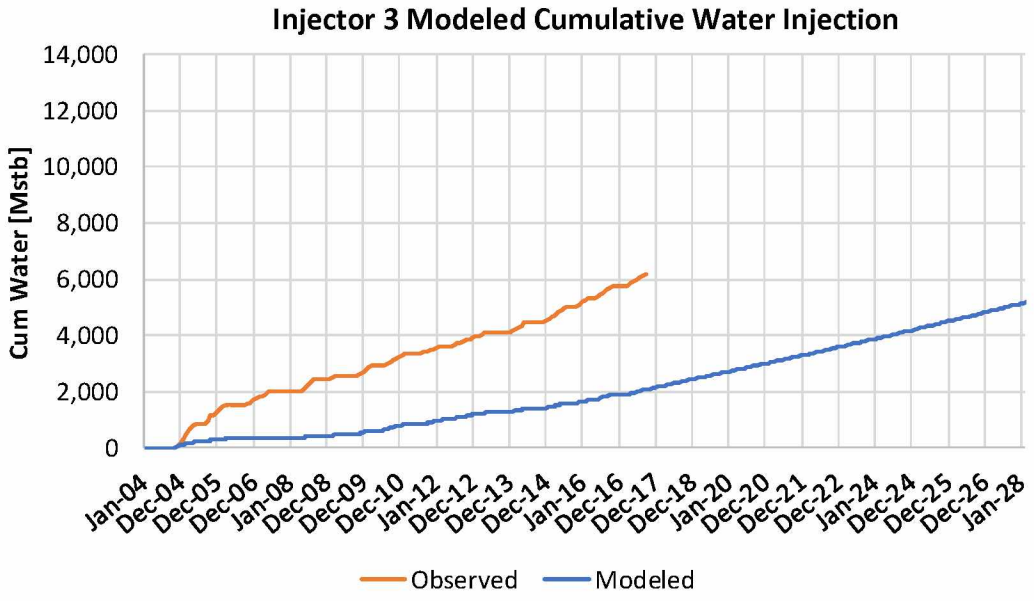

Figure 26: Injector 3 Cumulative Water Injection

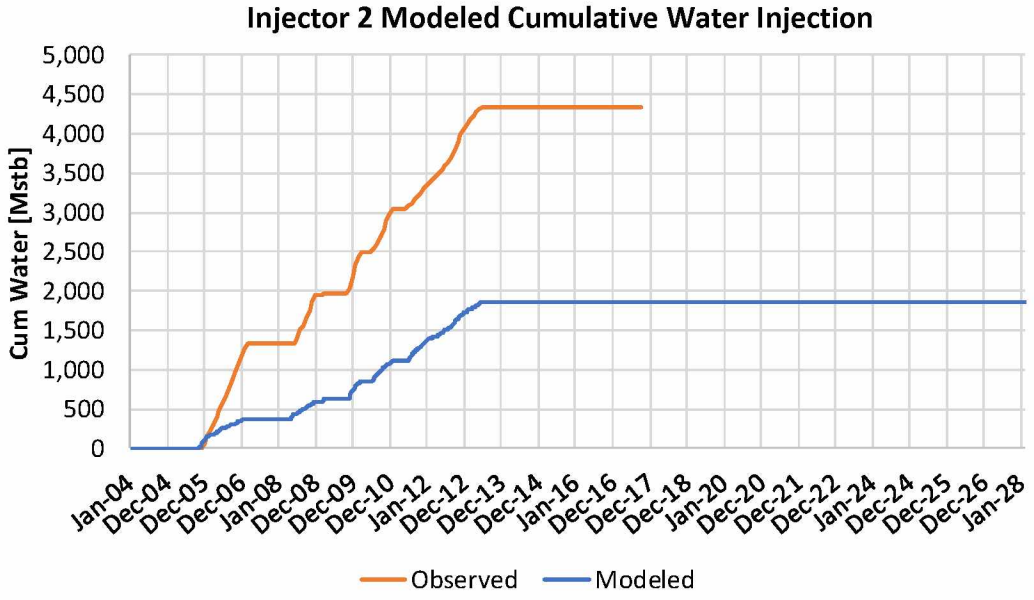

Figure 27: Injector 2 Cumulative Water Injection

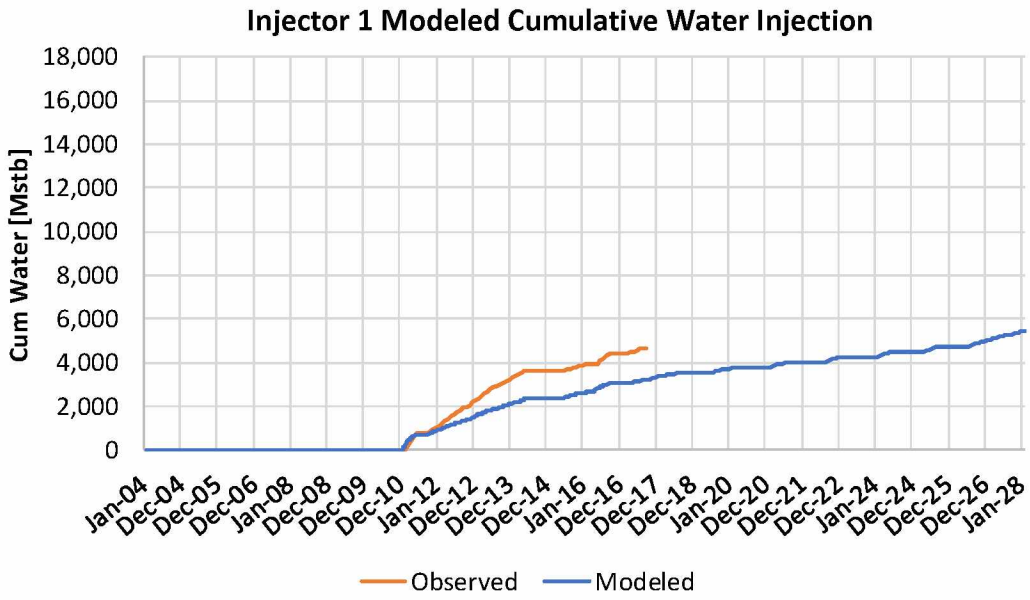

Figure 28: Injector 1 Cumulative Water Injection

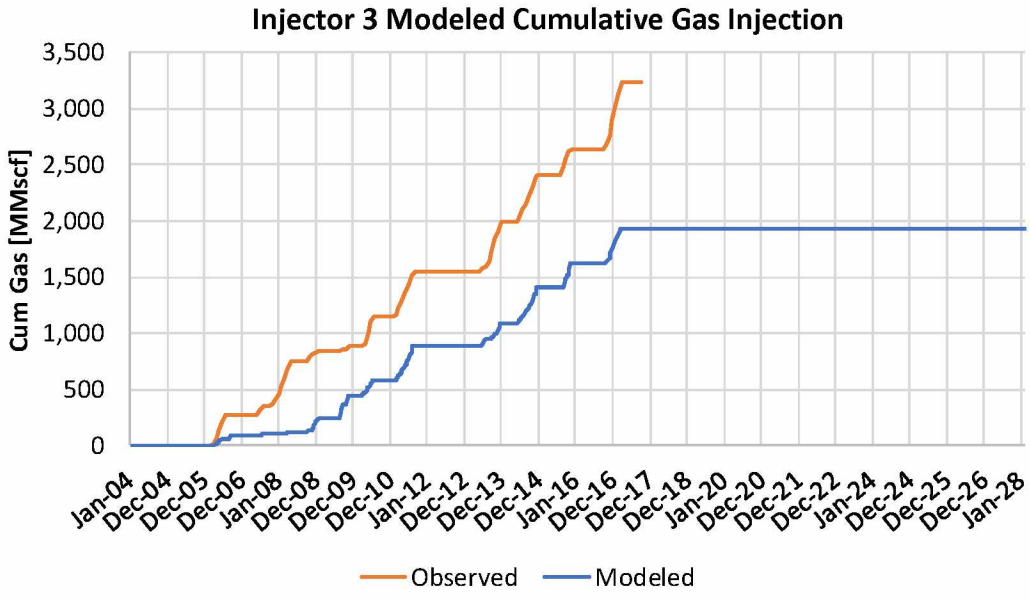

Figure 29: Injector 3 Cumulative Gas Injection

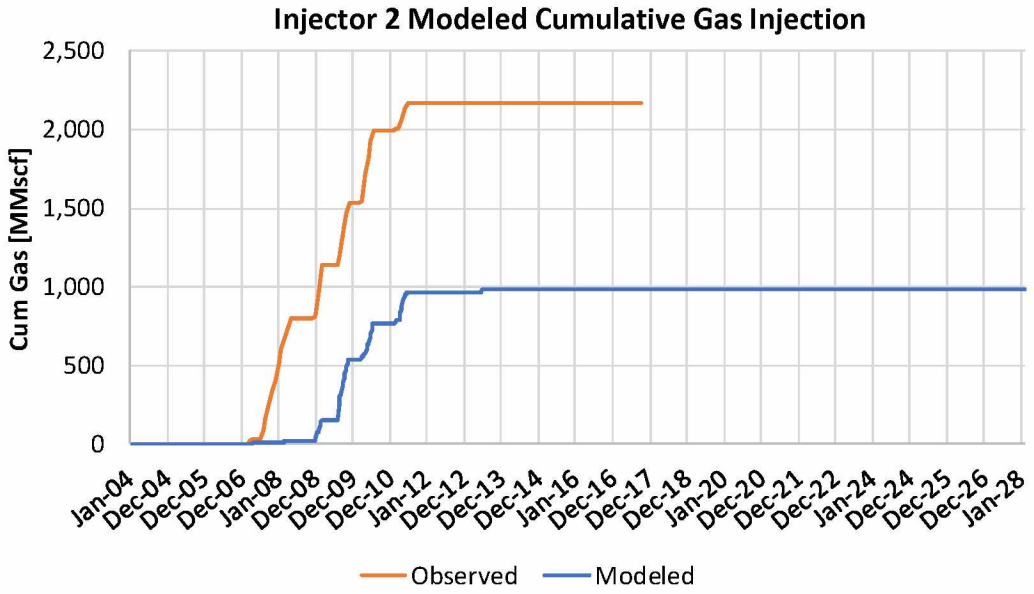

Figure 30: Injector 2 Cumulative Gas Injection

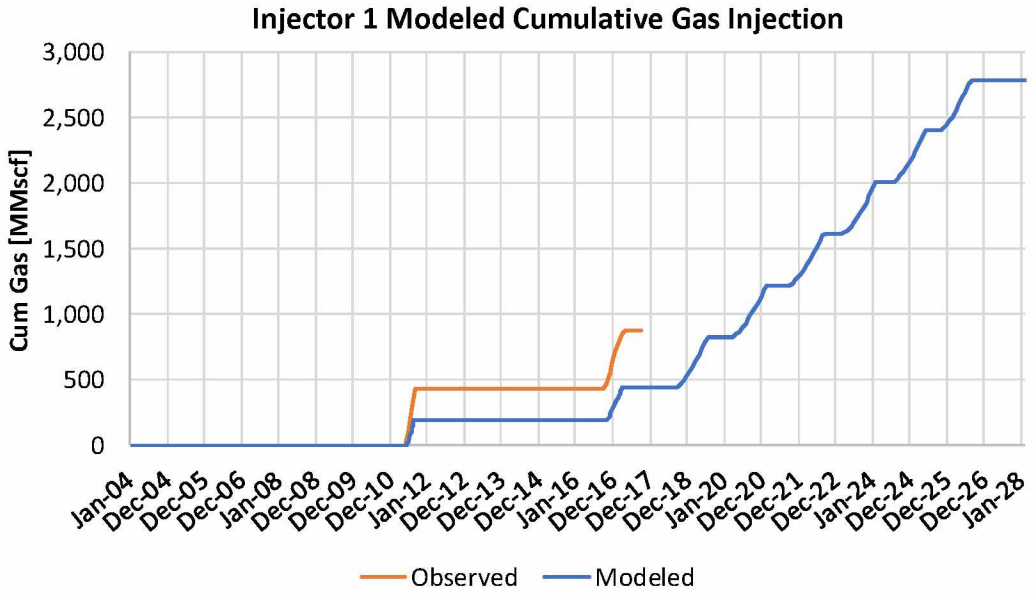

Figure 31: Injector 1 Cumulative Gas Injection

3.4. Modification of Type Pattern Model for IPR Study

The sector model described above was stripped of all scheduled 'events' for use in the IPR analysis, this allows us to isolate the mechanisms for the production process without burdening it with the complexities of injector shut-ins or producer fracture treatments.

4. Analysis of IPR Behavior

4.1. Validation of Bendakhlia Method for Creating IPRs

The Bendakhlia method for deriving an IPR curve from a numeric transient reservoir model was first introduced in the literature review section, here the proposed method will be described in detail and validated against a reservoir system similar to what Vogel used to originally develop his dimensionless IPR curve.

An IPR curve is the relationship between bottom hole pressure and flow rate at a specified recovery factor. Given a numeric model, the easiest way to calculate any single point on the IPR is to run that numeric model at the desired bottom hole pressure until the recovery factor specified for the IPR curve is achieved; this rate then becomes one point on the IPR curve. To fully describe the curve, you will need to run many different bottom hole pressure scenarios.

A numeric reservoir model was created with a vertical well completed in a sand with limited anisotropy and near homogenous permeability. The model is setup to produce with a solution gas drive mechanism so its resulting IPR curves will be directly comparable Vogel's reference curve. Figure 32 shows the setup of this model.

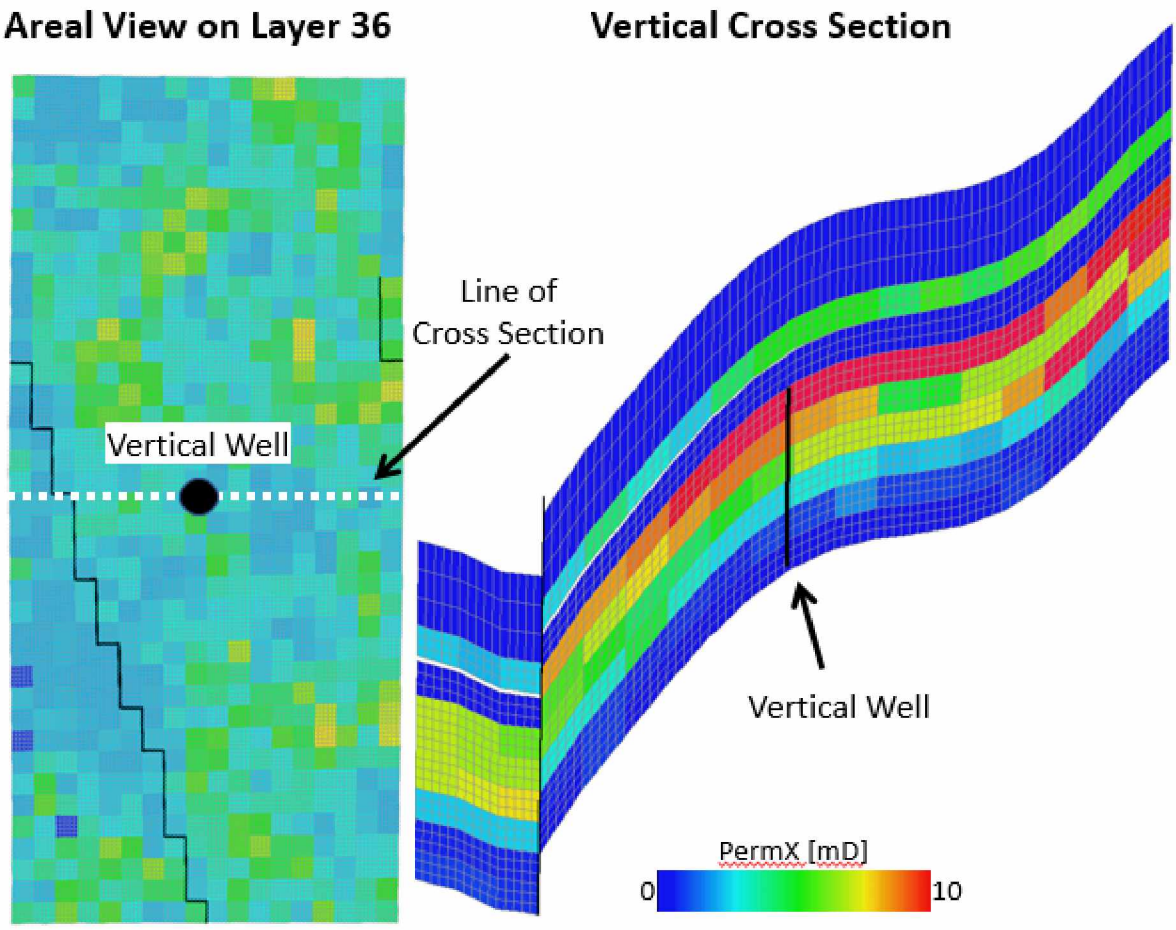

Figure 32: Setup of Vertical Well in Solution Gas Drive Reservoir

Figure 33 shows the oil rates calculated by the vertical well model for each constant bottom hole pressure case as a function of time, Figure 34 shows the same oil rate results as a function of the producer's recovery factor. An IPR curve at 12% recovery factor can then be determined by looking up the oil rate calculated for each bottom hole pressure case at a recovery factor of 12%.

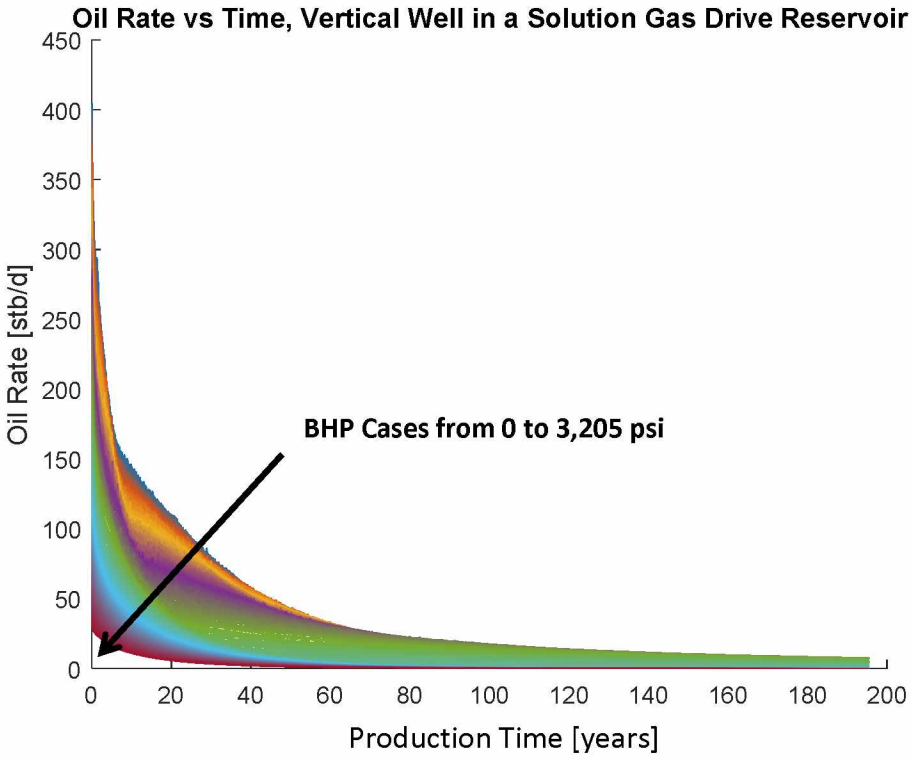

Figure 33: Oil Rates as a Function of Time for a Vertical Well in a Solution Gas Drive Reservoir

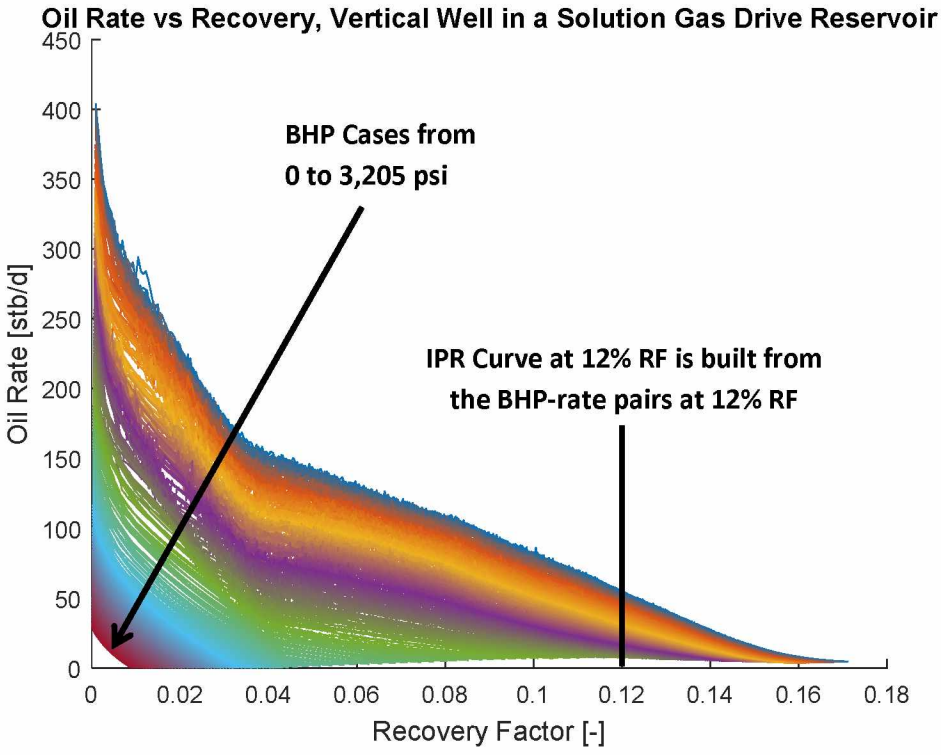

Figure 34: Oil Rates as a Function of Recovery for a Vertical Well in a Solution Gas Drive Reservoir

Figure 35 shows the resulting IPR curves over a range of recovery factors from 0.1% to 17%. Each circle along the IPR curves represents one model run, as the recovery factor specified for the IPR curve increases the number of bottom hole pressure cases capable of achieving that recovery factor is reduced. For instance, all 218 bottom hole pressure cases (i.e. every model run) is represented in the 0.1% IPR curve while the 17% curve contains only 9 cases representing bottom hole pressures from 0 to 80 psia. Each IPR curve is also fit with a Vogel (1968) and Fetkovich curve (1973). The Fetkovich 'n' fitting parameter was calculated by minimizing the sum of squares error against the numeric model derived curve; the calculated 'n' value for each IPR curve is specified next to its legend entry.

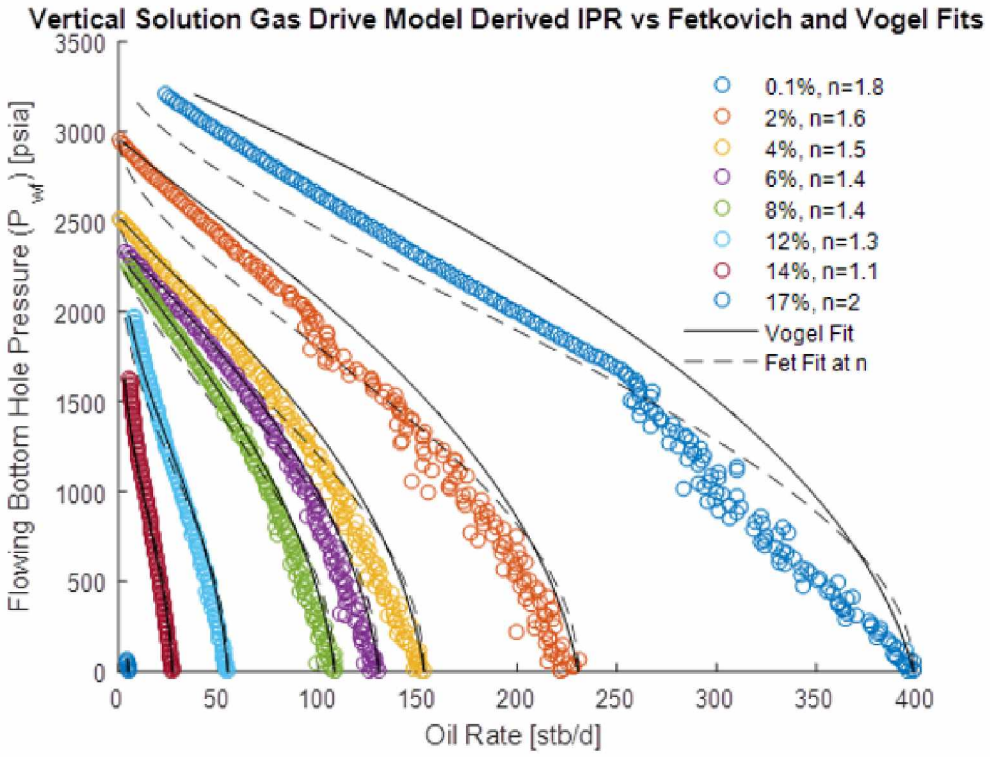

Figure 35: IPR Curves for a Vertical Well in a Solution Gas Drive Reservoir

If the curves are normalized in the method proposed by Vogel (1968) they collapse around his reference curve which is the behavior he observed when he originally proposed that IPRs in a solution gas drive reservoir could, with reasonable engineering error, be represented by a single curve. This result and the respective Fetkovich curves are displayed in Figure 36.

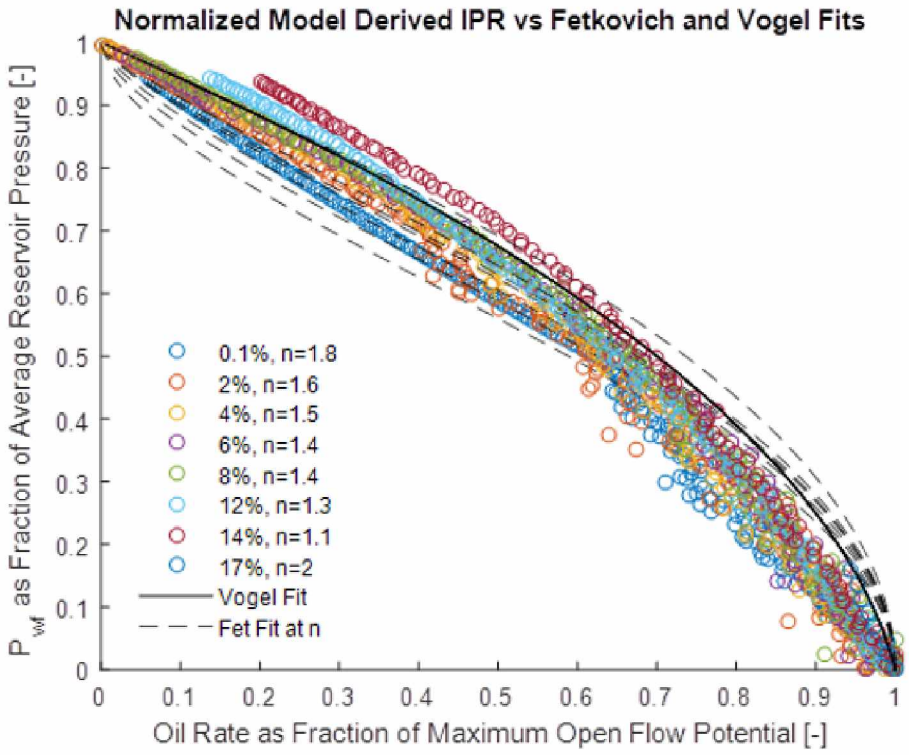

Figure 36: Normalized IPR Curves for a Vertical Well in a Solution Gas Drive Reservoir

The ability of the Bendakhlia method to recreate Vogel's result for a vertical well in a solution gas drive reservoir should give us confidence that the method can be extended to derive IPR curves for more complicated reservoir depletion methods.

4.2. Setup of Horizontal Waterflood and WAG Cases

Details on the setup of the model, gridding, wells, etc. can be found in Section 4. IPR curves have been generated for the A-sand under water flood and an EOR flood where enriched gas injection alternates with water injection. To simplify interpretation of the model results injection pressure, regardless of service, was set to a constant 5,000 psi. The water-alternating-gas injection schedule was standardized across all cases; an initial 10% pore volume (PV) slug of water is injected, followed by alternating slugs of 5%PV gas, then 5%PV water, until a total 30%PV slug of gas has been injected at which point the injector only injects water for the remainder of the model run.

4.3. Results of Water Flood Cases

The oil rates forecasted for the water flood supported horizontal well in the Alpine A-sand are shown below as a function of time in Figure 37 and a function of recovery factor in Figure 38. To complete the IPR curves back to the Y-intercept, bottom hole pressure cases needed to be run up to

the injector BHP of 5,000 psia. Since this is well above the initial reservoir pressure of 3,250 psia these high BHP cases have a period of time with zero flow rate. This is an abstraction of reality and represents an operating condition which is not practical or desired, but it does demonstrate the linearity of the IPR curve at high bottom hole pressures at the Y-intercept.

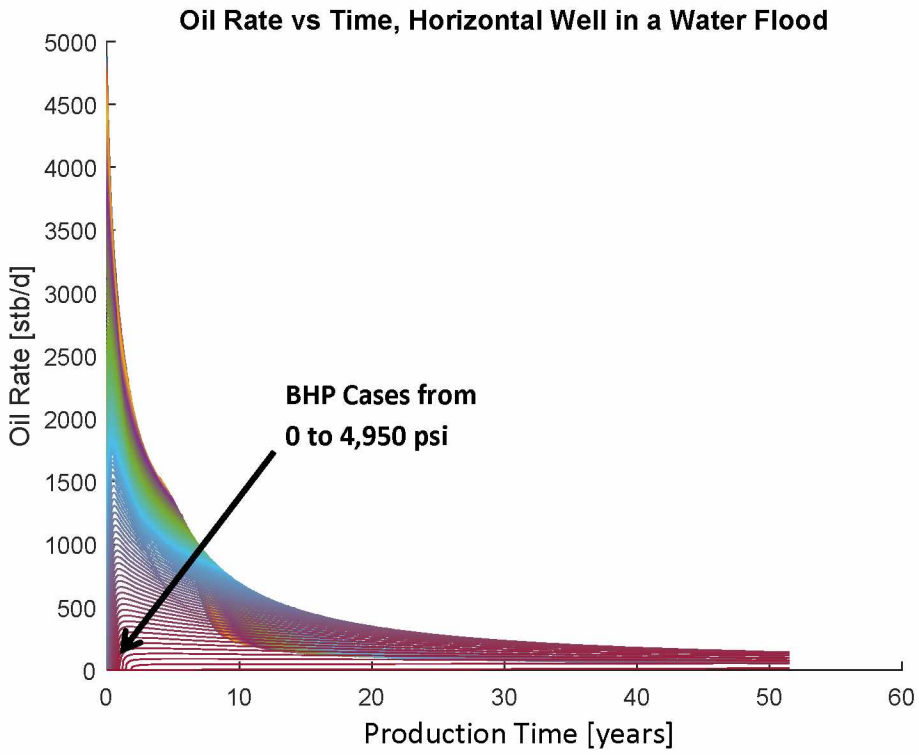

Figure 37: Oil Rates as a Function of Time for a Horizontal Well under Waterflood

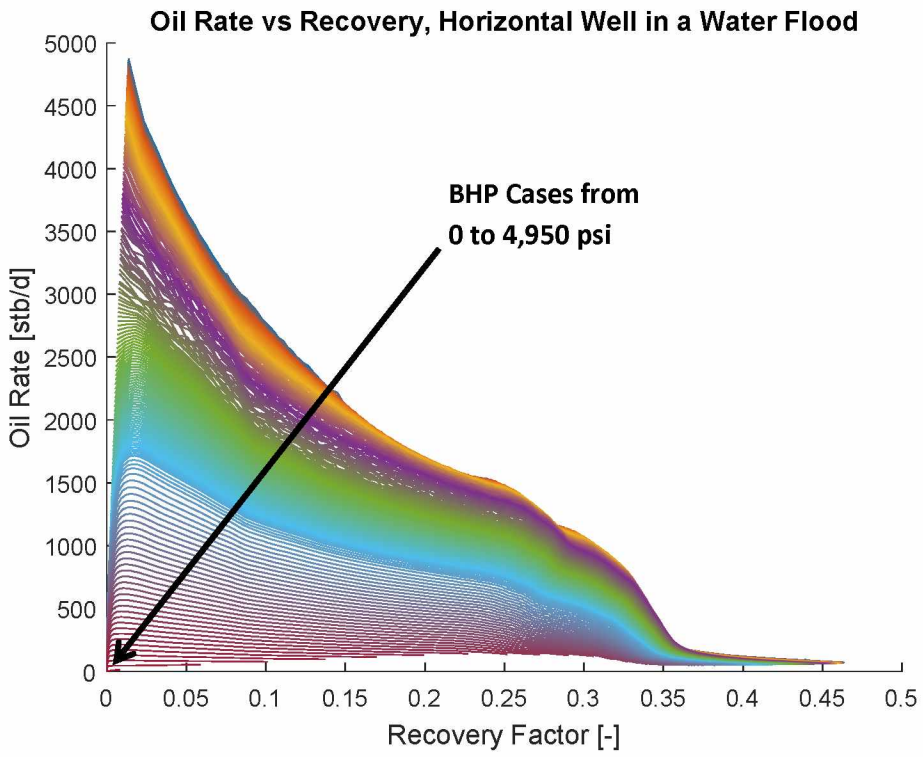

Figure 38: Oil Rates as a Function of Recovery for a Horizontal Well under Waterflood

The IPR curves resulting from the oil rates discussed above are shown in Figure 39 and Figure 40. As with the vertical well example the Vogel and Fetkovich curve fits for each IPR curve are shown. Each point along the IPR curve (represented as a colored circle) is a separate model run, 255 constant bottom hole pressure cases were run to describe with high fidelity the shape of the IPR curve at each specified recovery factor.

The calculated IPR curves differ from both the Vogel and Fetkovich fits; over the range of flowing bottom hole pressures typical for gas lifted wells, 1,000 to 2,000 psi, the calculated IPR curves have a much greater (steeper) slope. This difference will have a tremendous impact on the "optimized" IGOR gas lift solution outlined in Section 2. An inflection is noticeable for the IPRs with recovery factors greater than 20%. This inflection implies that, at the specified recovery factor, the highest oil rate is not being achieved at the lowest bottom hole pressure. The inflection becomes even more apparent in the normalized IPR plot.

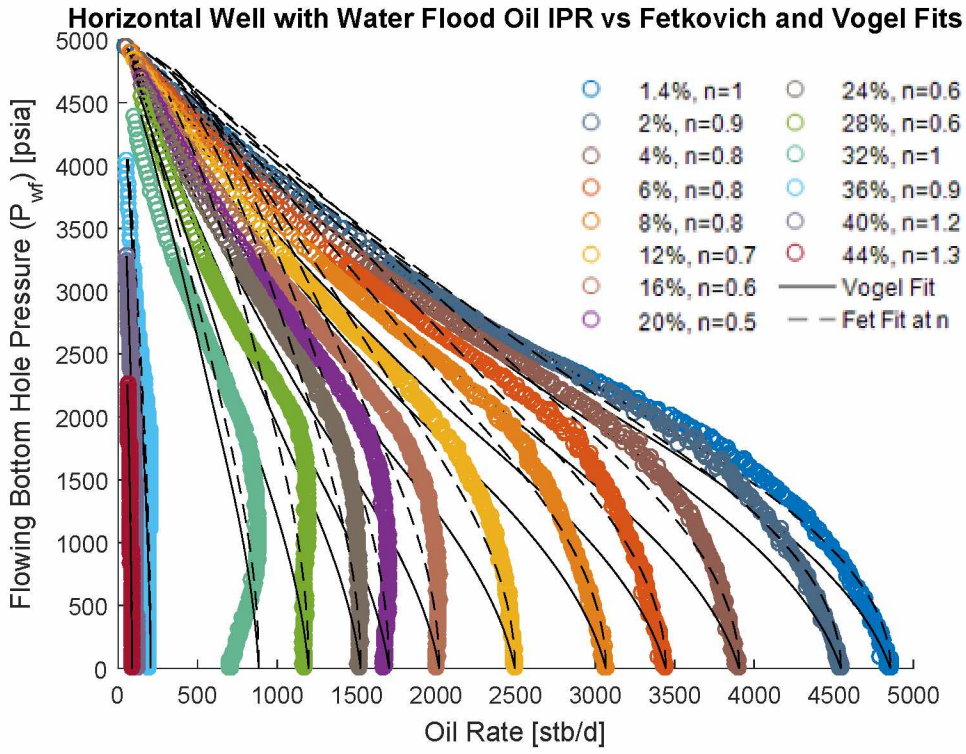

Figure 39: IPR Curves for a Horizontal Well in a Water Flooded Reservoir

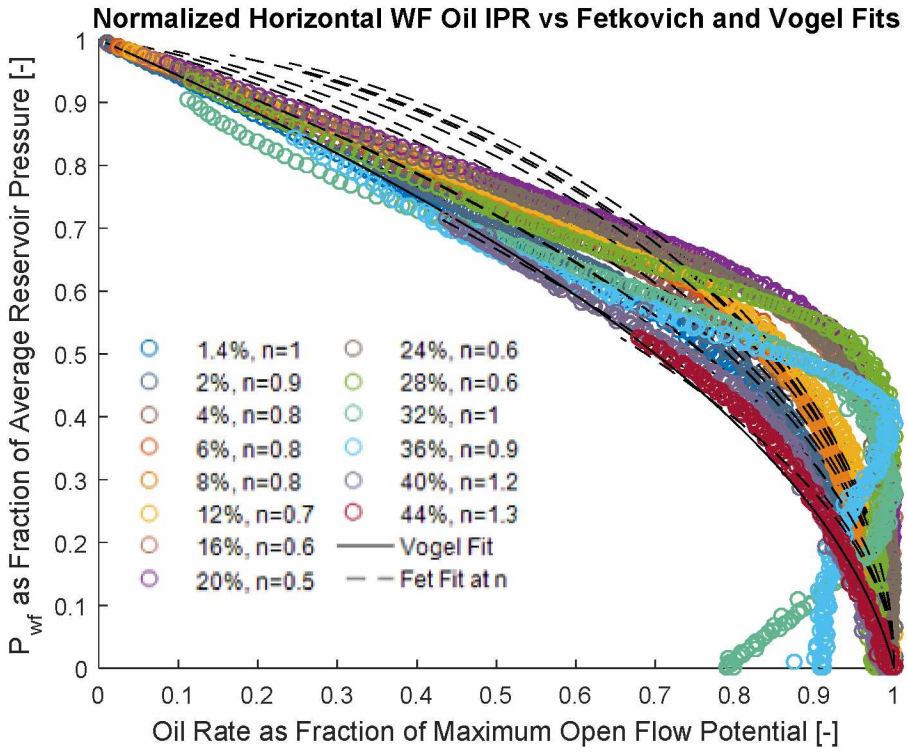

Figure 40: Normalized IPR Curves for a Horizontal Well in a Water Flooded Reservoir

Changing oil rate as a function of bottom hole pressure, at a constant recovery factor, necessitates a change in water flood performance also as a function of producer bottom hole pressure. If this is happening it should be readily apparent on a plot of dimensionless WOR performance. Figure 41 displays this performance for four bottom hole pressure cases: 0; 1,000; 2,005; 2,500; and 2,725 psi. The performance of the 2,725 and 2,500 psi cases is almost identical and this holds for all other cases where the bottom hole pressure is greater than the fluid's 2,500 psi bubble point. As the bottom hole pressure drops below the bubble point the WOR performance begins to change. Initially, between 2,500 and 2,000 psi, it is marginally improved, the curve shifts right, and the arrival of significant water volumes is slightly delayed. As the bottom hole pressure is further decreased the curve begins to shift back to the left (2,005 to 1,000 psi), below 1,000 psi the WOR performance exhibits a non-linear response with a large shift left to the 0 psi case.

The most significant driver of the observed change in flood behavior appears to be the reciprocal increase in gas production as the bottom hole pressure is decreased, this is shown in Figure 42.

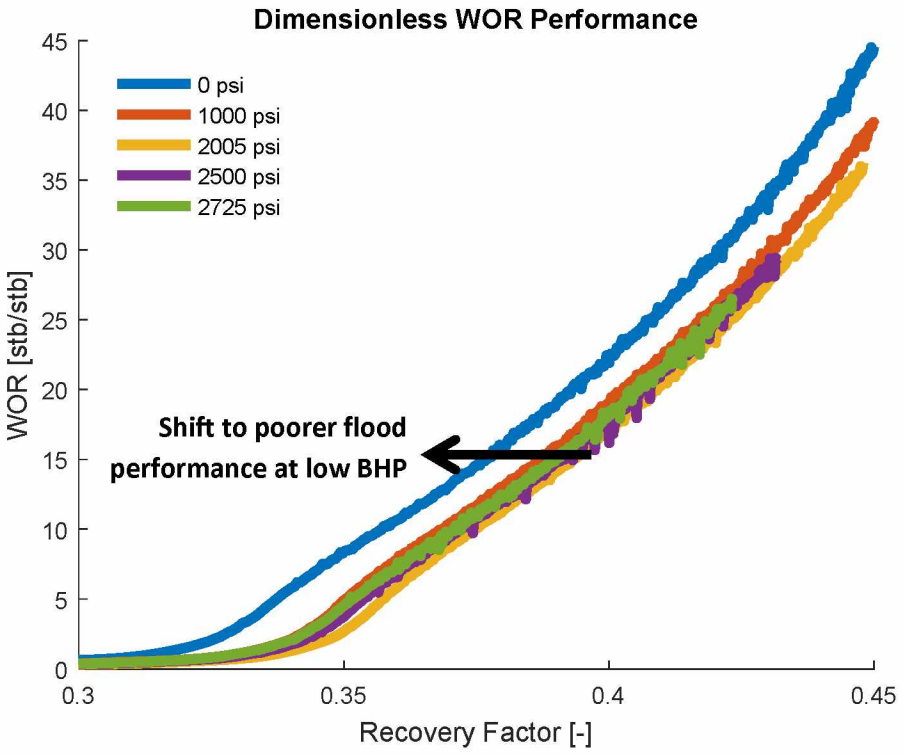

Figure 41: Water Flood Performance Changes with Producer Bottom Hole Pressure

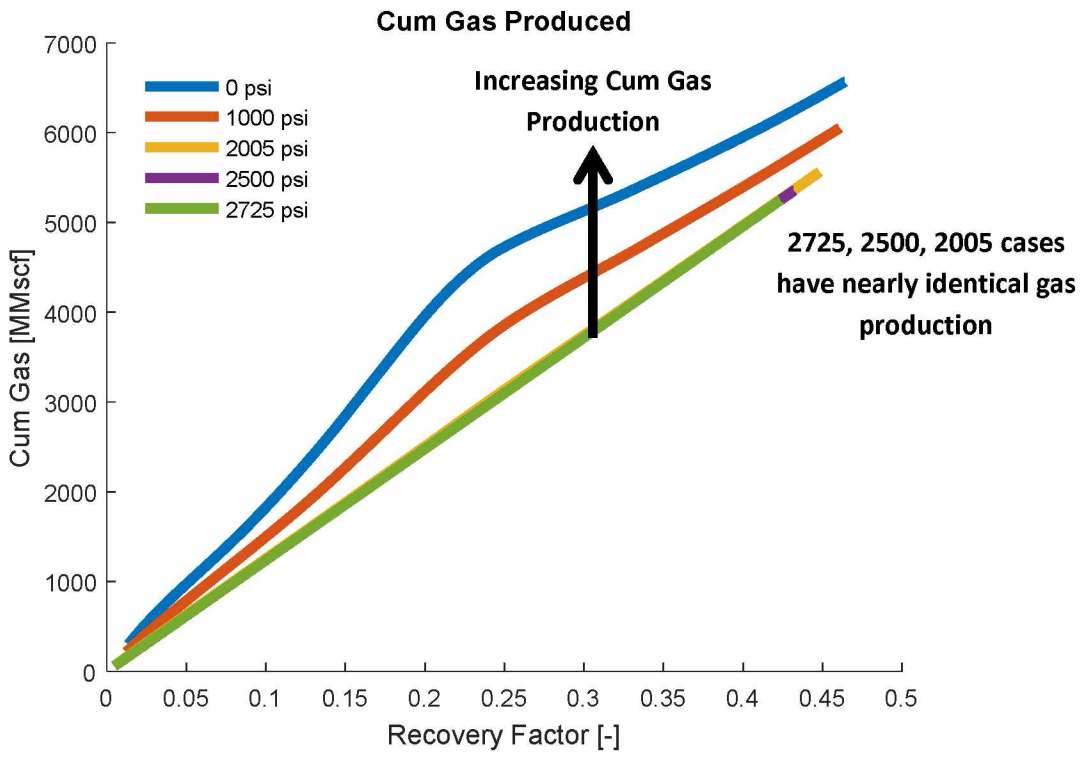

Figure 42: Cumulative Gas Production for Selected BHP Cases of a Horizontal Well under Waterflood

The reduction of dissolved gas in the oil phase has the detrimental effect of increasing its viscosity and decreasing its mobility; the decreased oil mobility of the lower BHP cases reduces the sweep efficiency of the water flood, shifting the WOR performance curve to the left.

4.4. Results of WAG Cases

As with the water flood cases we'll begin with a display of oil rate for each bottom hole pressure case as a function of time in Figure 43 and recovery factor in Figure 44.

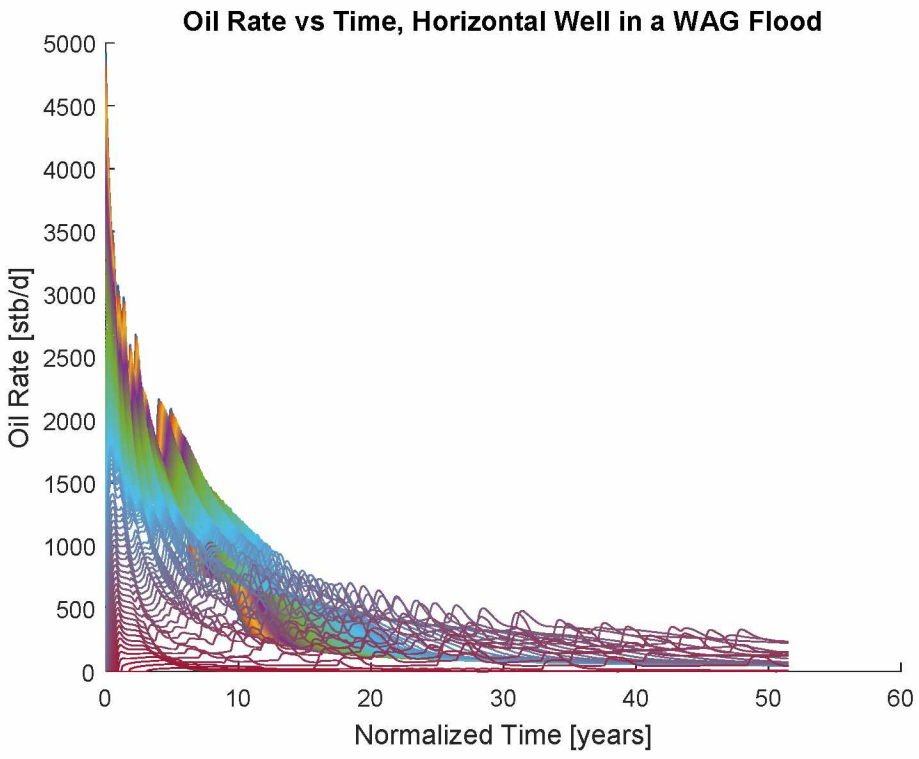

Figure 43: Oil Rates as a Function of Time for a Horizontal Well under WAG Flood

Figure 44: Oil Rates as a Function of Recovery for a Horizontal Well under WAG Flood